Relaxation phenomenon and swelling behavior of cellulose fibers affected by water and organic solvents

2019

KOBE WOMEN'S UNIVERSITY

GRADUATE SCHOOL OF HOME ECONOMICS

AKARI OKUGAWA

Contents

Abstract..... 4

Chapter 1..... 5

1.1. Introduction..... 5

1.2. Wettability of regenerated cellulose..... 8

1.3. Post-treatment to reduce the effects of water on cellulose fibers.....11

1.4. Aim of this study.....13

Reference.....14

Chapter 2. Relaxation phenomenon and swelling behavior of regenerated cellulose fibers affected by water.....17

2.1. Introduction.....17

2.2. Materials and Methods.....20

2.2.1. Materials.....20

2.2.2. Dynamic Viscoelasticity.....20

2.2.3. Tensile strength and elongation.....20

2.2.4. Wide angle X-ray scattering (WAXS).....21

2.2.5. Small angle X-ray scattering (SAXS).....21

2.3. Results and Discussion.....23

2.3.1. Relaxation phenomenon of regenerated cellulose fibers.....23

2.3.2. Swelling behavior of regenerated cellulose fibers.....30

2.4. Conclusions.....35

Chapter 3. Relaxation phenomenon and swelling behavior of regenerated cellulose fibers affected by organic solvents.....39

3.1. Introduction.....39

3.2. Materials and Methods.....40

3.2.1. Materials.....40

3.2.2. Dynamic Viscoelasticity.....40

3.2.3. Small angle X-ray scattering (SAXS).....40

3.3. Results and Discussion.....42

3.3.1. Relaxation phenomenon of regenerated cellulose fibers by organic solvents.....42

3.3.2. Swelling behavior of regenerated cellulose fibers by organic solvents.....46

3.4. Conclusions.....49

References.....50

Chapter 4. Relaxation phenomenon and swelling behavior of natural cellulose fibers affected by water.....53

4.1. Introduction.....53

4.2. Materials and Methods.....55

4.2.1. Materials.....55

4.2.2. Dynamic Viscoelasticity.....55

4.2.3. Small angle X-ray scattering (SAXS).....55

4.3. Results and Discussion.....57

4.3.1. Relaxation phenomenon of natural cellulose fibers.....57

4.3.2. Swelling behavior of natural cellulose fibers.....60

4.4. Conclusions 65

References 66

Chapter 5. Conclusion 67

List of publication 71

Acknowledgments 72

Abstract

Regenerated cellulose fibers are extremely sensitive to water. In order to solve this problem and develop their advantages, the effect of water and organic solvents on cellulose fibers in respect of the relaxation phenomenon and swelling behavior was examined. The glass transition temperature of regenerated cellulose fibers could be decreases to room temperature by immersion in water and various organic solvents, which was estimated from the shift of peaks and shoulders of mechanical loss tangent δ (tan δ) in dynamic viscoelastic behavior. However, this glass transition did not occur in alkanes lager than nonane, which are the main component of petroleum based dry cleaning solvents. This suggested that the remarkable wrinkles and shrinkage of regenerated cellulose fibers due to home-washing were caused by the molecular motion of the cellulose main chains. Regenerated cellulose absorbs water and organic solvents and then swells. This swelling is closely related to the molecular movement revealed by small-angle X-ray scattering of high-intensity synchrotron radiation in addition to the measurement of dynamic viscoelasticity and mechanical properties. Furthermore, these phenomena were also observed for natural cellulose fibers such as cotton and ramie; however, effect of water on natural cellulose fibers was extremely smaller than that on regenerated cellulose fibers. If the effects of water on the regenerated cellulose fibers could be suppressed to the level of natural cellulose, a great shortage of cotton supply expected in the near future could be filled with newly designed regenerated cellulose fibers.

Chapter 1

1.1. Introduction

Cellulose is the main component of plants, accounting for about 40～50% of their dry weight, and is the biological resource that is most predominantly produced and accumulated on the earth by photosynthesis. Cellulose does not have a crystalline melting point until its decomposition; in order to form films, fibers, hollow fibers, sponge and spheres according to the application, it must be dissolved in solution and precipitated. Such structures are defined as regenerated cellulose. The dissolution systems to produce regenerated cellulose on an industrial scale are the cuprammonium method (cupra for textile fibers) and the viscose method (rayon for textile fibers), which were developed in the late nineteenth century; at that time, the concept of polymers had not yet been established. Another system is the *N*-methyl morpholine *N*-oxide (NMMO)/water system (lyocell for textile fibers), which was developed in the 1980s. The main problems of the former two dissolution systems are emission of heavy metals and carbon disulfide. This is the probable reason that new dissolution systems (mainly using ionic liquids) are still being pursued, as described below.

Rogers and his colleagues recently rediscovered ionic liquid (IL) as a powerful cellulose solvent, and this led to a new research field aiming to substitute previous systems for manufacturing regenerated cellulose and create next-generation fibers[1)]. Ionic liquids (ILs) have proven to be effective cellulose solvents, as they can dissolve cellulose without heating. Initially, the ILs used to prepare the spinning dope were all imidazolium based. These ILs can more easily control the direct dissolution of cellulose when compared to the NMMO process. In addition, this process is inherently safe and has been shown to yield fibers with properties comparable to those produced from NMMO solutions[2, 3)]. However, imidazolium-based ILs slightly degraded cellulose[4)]. Stabilizers were added depending on the substituents of the imidazolium ring and the chemical nature of the anion to prevent cellulose degradation, particularly at high temperatures (> 90°C). The anions of first-

generation ILs were usually a halogen compound that is highly corrosive to metal processing equipment[5]. Then, acetate as the anion species was applied; specifically, 1-ethyl-3-methylimidazolium acetate was used as a cellulose solvent, where the resulting cellulose solution is obtained with low viscosity. However, viscoelastic properties suitable for stable spinning can only be achieved in a very narrow concentration range. Optimal spinning can be achieved by increasing the cellulose concentration to 20 wt%[6].

In recent years, a new cellulose spinning solvent consisting of superbase/acid ion pair has been developed in the search for efficient non-imidazolium-based cellulose solvents[7]. 1, 5-Diazabicyclo [4.3.0] non-5-enium acetate was appropriate among the superbase-based ILs, and an air gap spinning system with this solvent created new regenerated cellulose fibers[8]. This new dry jet wet spinning process is called the Ioncell-F process, and the manufactured fibers are called Ioncell-F fibers. This fiber has been successfully made into a textile similar to that produced by the NMMO/water system. However, this series of studies of regenerated cellulose fibers only focused on improving mechanical practical properties such as strength, elongation, and Young's modulus. It remains unclear what properties and structure are required for next-generation fibers.

The production ratio of man-made cellulose fibers such as rayon, cupra, and lyocell including acetate fibers, to global fiber production was approximately 6% in 2017. However, regenerated cellulose is readily affected by water, and washing with water causes significant wrinkling, shrinkage, and fibrillation, resulting in an extremely limited market, due to the necessity of dry cleaning for finished products. Meanwhile, the cotton gap is a mid- to long-term issue related to fiber materials[9]. This cotton gap is a large gap between supply and demand for cotton that will occur in the near future. Although the demand for cotton is increasing year by year due to the worldwide increasing population and economic development in developing countries, the production capacity for cotton has already reached its limit, as grain fields are prioritized in the adaptation for food source, and the number of fields themselves are decreasing due to the impact of urbanization, and concerns about the large amount of pesticides required for cotton cultivation affecting the

surrounding environment. Regenerated cellulose fibers have the potential to fill a large gap between the demand and production capacity of such cotton, rather than polyester fibers. Regenerated cellulose fibers are made of the same material (cellulose) as cotton, and they offer the possibility of developing fibers with properties that exceed those of cotton. However, fibers that cannot be washed at home are not a substitute for cotton. If a regenerated cellulose fiber is developed that can control the hydrophilicity of the regenerated cellulose and fill the cotton gap, a large market will be opened. These situations raise the question of why regenerated cellulose is so markedly affected by water.

Regenerated cellulose has long been used as a dialysis membrane for artificial kidneys in addition to textile fibers. However, it was completely replaced with a dialysis membrane made of synthetic polymers due to problems with biocompatibility. Regenerated cellulose causes a phenomenon called leukopenia, in which the number of leukocytes decreases rapidly at the beginning of dialysis, because hydroxyl groups present on the surface of the regenerated cellulose activate the complement. As a solution, the activation of complement was suppressed by blocking the hydroxyl group using a polyethylene glycol with an alkyl group at the end. Nevertheless, the effects were limited, and the regenerated cellulose artificial kidney disappeared. This indicates that there are many accessible hydroxyls on the regenerated cellulose and its uses are limited.

Conversely, regenerated cellulose foods produced with aqueous sodium hydroxide solution are extremely sensitive to water. For food applications, it is good that the regenerated cellulose has high water absorption and that the elastic modulus and strength are reduced by water. Regenerated cellulose from aq. NaOH solution is legally edible among the other types of regenerated cellulose, as the chemicals used in this process are only sodium hydroxide for dissolution and sulfuric acid for coagulation. This new functional food is categorized as Generally Recognized as Safe substances by the United States Food and Drug Administration. Furthermore, this first cellulose food in the world is free of calories and is expected to meet the needs of modern society to prevent lifestyle-related diseases.

1.2. Wettability of regenerated cellulose

Regenerated cellulose has an immutable feature, in that regenerated cellulose is extremely sensitive to water and is classified as one of the most hydrophilic polymers, having an extremely wettable surface. The hydrophilicity of cellulose is due to three hydroxyls per anhydroglucose unit; however, this alone cannot reasonably explain why its wettability is so high. The contact angles of water droplets on cellophane (prepared by the viscose method) and cuprophane (prepared by the cuprammonium method), which are typical regenerated cellulose films, are shown to be 11.6° and 12.2°, respectively. These angles are far lower than those of widely used polymers. Although the hydrophilic polymer (poly vinyl alcohol, PVA), which contains many hydroxyls, has a low contact angle (36°), this value is still higher than that of regenerated cellulose films. It is notable that the contact angle of water on starch film, which is highly soluble in hot water, is 41°. The high wettability of regenerated cellulose films could be attributed to the higher density of hydroxyl groups on a cellulose surface than on the PVA surface; the densities of hydroxyls on the film surfaces of cellophane and PVA are 1×10^{-5} and 5×10^{-6} mol m^{-2}, respectively[10]. Why is the hydroxyl density on the surface of regenerated cellulose high?

Cellulose is an intrinsically amphiphilic polymer in its primary structure[11-13], which has hydrophilic and hydrophobic anisotropy. β-Glucopyranose with $^4C_1$ ring conformation has a hydroxyl group in the equatorial direction, and this direction is hydrophilic, but the axial direction is hydrophobic due to the presence of C-H hydrogen atoms. If these hydrophilic parts are evenly aligned, a very hydrophilic surface could be created. Here, natural cellulose is a crystal form of cellulose I, and regenerated cellulose is cellulose II. In cellulose II, the cellulose along the $(1\bar{1}0)$ plane is aligned by hydrophobic (not hydrogen-bonded) interactions, resulting in a concentration of hydroxyl groups on the surface of the $(1\bar{1}0)$ plane. Therefore, it is expected that the surface energy of the $(1\bar{1}0)$ plane is high and water readily approaches. It has been confirmed that the surface energy of the $(1\bar{1}0)$ plane is the highest among all crystal planes of cellulose I and II polymorphs, which was estimated by a molecular dynamics simulation[14]. The high water wettability of

regenerated cellulose is caused by $(1\bar{1}0)$ plane orientation of $(1\bar{1}0)$ parallel to the film surface detected by wide-angle X-ray diffraction[14, 15]. Although the contact angles of water droplets are greatly affected by surface roughness, it has been confirmed that the surfaces of all these films are smooth. The contact angles of water droplets decrease with the increases in crystallinity and the plane orientation index. Thus, the density of hydroxyl groups on the surface probably increases as the crystallinity and the plane orientation index increase, and leading to easier access of water.

Regenerated cellulose is readily wetted not only on the surface, but also internally. The range of the swelling ratio of regenerated cellulose is 50-200%. The swelling ratio is defined as the ratio of the weight/weight percentage (w/w %) of water that remains in fibers after centrifugation at 1,000 × *g*, to dry weight. Water probably penetrates into the region between the micro-fibrils (train of crystals); then the space between micro-fibrils widens and density decreases. The films with the uniplanar orientation of $(1\bar{1}0)$ crystal plane parallel to the film surface were also immersed in water, and the thickness expanded about two-fold, but the area did not change[16]. Thus, it is suggested that water infiltrates along the $(1\bar{1}0)$ crystal plane oriented parallel to the film surface, and that the inside of the film also has a wettable surface.

When cellulose that has been molecularly dispersed in a solution begins to coagulate, glucopyranose rings are stacked together by hydrophobic interactions and van der Waals forces, as cellulose solvents and coagulation systems are aqueous or highly polar solvent systems; molecular sheets are then formed[17]. Molecular sheets have a hydrophobic interior and hydrophilic periphery with many hydroxyls, and also must be a fundamental structure of regenerated cellulose. The formation of such molecular sheets at the initial stage of coagulation was confirmed by time-resolved observation of high-intensity synchrotron X-ray radiation[18], and increasing thickness of the molecular sheet by time-resolved thickness Guinier plot[19]. In addition, the molecular dynamics simulation confirmed the stability of the molecular sheet as a starting structure in water. This molecular sheet is hydrophobic in its interior and could be present stably, like the micelles

of surface active agents in water, as the surface of the molecular sheet has a high hydroxyl density. These molecular sheets are then presumably stacked by hydrogen bonds to form thin planar crystals incorporating amorphous chains; after that, these randomly dispersed structures in the solution make contact with and adhere to one another to form three-dimensional structures. Here, it is considered that a region stacked uniformly without distortion becomes a crystal, and a region stacked with strain and distribution in the distance between sheets becomes an amorphous region. Hydrophilic surfaces with many accessible hydroxyls are consequently formed[20]. Therefore, the basic structure of regenerated cellulose would be this molecular sheet. This sheet has been referred to by some researchers as a "sheet like structure", "the form of lamellae" or "the lamellar plane"[21-23].

As noted above, the surface of the molecular sheet has a high hydroxyl group density and is extremely hydrophilic. It is inevitable that regenerated cellulose is easily affected by water as it is a stack of structural units having a hydrophilic surface. A possible approach to control the hydrophilicity of regenerated cellulose is to create a molecular sheet formed with hydrogen bonds at the early stages of coagulation, thereby resulting in hydrophobic cellulose with many hydrogen atoms of C-H bonds on its surface. Computational studies have demonstrated the formation of a hydrogen-bonded molecular sheet as the initial structure in a benzene environment[17]. However, it is not practical because regenerated cellulose cannot actually be produced in a non-polar state. This approach was successful for regenerated chitin prepared from the DMAc/LiCl solution system[20]. It is expected that this principle will be elucidated and applied to cellulose in the near future. As described above, it has been clarified that the high wettability of regenerated cellulose and the characteristics that are too sensitive to water are determined at the initial stage of structure formation.

On the other hand, the cause of wrinkles and shrinkage due to water, which is the greatest drawback of regenerated cellulose fibers, has not been clarified. The wet moduli of regenerated cellulose fibers are markedly lower than those of conditioned moduli; the

ratios of wet/conditioned moduli were 1/24, 1/6, and 1/13 for rayon, cupra and lyocell, respectively[24], suggesting that some segmental movements in cellulose main chains are released in the wet state. In addition, although regenerated cellulose is essentially an amphiphilic polymer, it can be dry-cleaned, and natural cellulose fibers with the same molecular structure can be washed with water; thus, it is necessary to investigate the effects of organic solvents and natural cellulose fibers on dynamic viscoelasticity and to investigate the relationship with swelling behavior. Based on this, it is necessary to elucidate the molecular motion state of regenerated cellulose caused by various solvents and the essential causes of the high hydrophilicity of regenerated cellulose.

1.3. Post-treatment to reduce the effects of water on cellulose fibers

As described above, the greatest problem of regenerated cellulose is marked wrinkling, shrinkage, and fibrillation by washing with water. Even for cotton, washing with water causes relatively minor shrinkage and wrinkling when compared to regenerated cellulose. These disadvantages can be suppressed to some extent by resin processing, liquid ammonia processing, and high-pressure steam processing in the case of cotton fibers.

Resin processing develops form stability by crosslinking the hydroxyl group (OH group) in the non-crystalline region of cellulose with a bifunctional resin agent. In this process, the fabric is impregnated with a solution containing a resin agent, and the fabric is then dried and heat-treated. This resin processing can be expected to improve shape stability by selecting resin agents or acidic catalysts, optimizing conditions such as reaction temperature or time and pretreatment. An important aspect of this process is that the non-uniform distribution of parts causes a significant decrease in strength, so that efficient and uniform cross-linking provides high shape stability performance. The resin

is generally an *N*-methylol compound. This resin processing has been used as an anti-wrinkle process for cellulose such as cotton since the beginning of the 20th century, and it has been used for modification aimed at wash-and-wear properties (W & W) since about 1960. However, resin processing on cotton fibers has the problem of reducing strength and making the fabrics stiff. This problem has been greatly improved since the introduction of liquid ammonia processing.

Liquid ammonia processing prevents swelling of the fiber core and modifies it into a relaxed state by instant pervaporation of liquid ammonia at ultra-low temperature to rearrange cellulose molecules. Thereby, the decrease in strength from resin processing can be reduced. As a pretreatment for a similar purpose, there is mercerization (a method of immersing in about 20 wt% sodium hydroxide solution), but liquid ammonia processing is more effective for modification. Although this method was initially used for only polyester and cotton blend fabrics, Nisshinbo Holdings Inc. in Japan, released a 100% cotton W & W product in 2009, incorporating improvements in resin processing technology[25]. However, these methods are difficult to apply to regenerated cellulose fibers because the effect of water is strong for regenerated cellulose, and it is necessary to pursue new resins and processing methods to solve these problems.

High-pressure steam treatment was developed by Tokai Senko K. K. to fix the shape of cotton cloth, and is known as "J-Wash"[26]. The treatment increases crystallinity, partially hydrolyzes amorphous regions, and thermally rearranges the amorphous regions into crystals. Although this method is effective for cotton, high-pressure steam hardly achieves the effect of shape fixing for regenerated cellulose, as regenerated cellulose is more sensitive to water than cotton. The tire cord rayon that is continuously heat-treated with high-temperature and high-pressure water could reduce the degree of swelling to about 1/1.6, which is close to that of cotton yarn, with almost no depolymerization or only a slight decrease in the degree of polymerization. The mechanical performance was not deteriorated by this method, and the tensile strength and elongation can be improved by the treatment. However, it has been reported that viscose rayon for clothing does not

provide a sufficient decrease in swelling[27].

As described above, these post-treatments alone are not sufficient to change the extreme sensitivity to water of regenerated cellulose. Therefore, it is necessary to clarify the relationship between dynamic viscoelastic behavior and swelling behavior of regenerated cellulose fibers and natural cellulose fibers with water and organic solvents, and to elucidate the molecular motion state of regenerated cellulose caused by water and various solvents to prevent the excessive wetness of regenerated cellulose.

1.4. Aim of this study

In this study, the dynamic viscoelastic behavior caused by water and various solvents and the related swelling phenomena for regenerating cellulose and natural cellulose were clarified. Based on these works, we aimed to elucidate the properties of regenerated cellulose that are significantly affected by water for the purpose of sustainable use of regenerated cellulose. The long-term goal is to develop regenerated cellulose fibers that exceed the properties of cotton, allowing us to control the hydrophilicity of regenerated cellulose.

Reference

1) Swatloski, R. P., Spear, S. K., Holbrey, J. D. and Rogers, R. D.: Dissolution of Cellose with Ionic Liquids, J. Am. Chem. Soc. 124(18), 4974-4975 (2002).

2) Bentivoglio, G., Roeder, T., Fasching, M., Buchberger, M., Schottenberger, H. and Sixta, H.: Cellulose processing with chloride-based ionic liquids, Lenzinger Ber. 86, 154-161 (2006).

3) Laus, G., Bentivoglio, G., Schottenberger, H., Kahlenberg, V., Kopacka, H., Roeder, H., Roeder, T. and Sixta, H.: Ionic liquids: current developments, potential and drawbacks for industrial applications, Lenzinger Ber. 84, 71-85 (2005).

4) Ebner, G., Schiehser, S., Potthast, A. and Rosenau, T.: Side reactions of cellulose with common 1-alkyl-3-methylimidazolium-based ionic liquids Tetrahedron Lett. 49(51), 7322-7324 (2008).

5) Cai, T., Zhang, H., Guo, Q., Shao, H. and Hu, X.: Structure and properties of cellulose fibers from ionic liquids, J. Appl. Polym. Sci. 115, 1047-1053 (2010)

6) Kosan, B., Michels, C. and Meister, F.: Dissolution and forming of cellulose with ionic liquids, Cellulose (Dordrecht, Neth.) 15, 59-66 (2008).

7) Michud, A., King, A., Parviainen, A., Sixta, H., Hauru, L., Hummel, M. and Kilpeläinen, I.: Process for the production of shaped cellulose articles from a solution containing pulp dissolved in distillable ionic liquids, FI Patent Application PCT/FI2014/050238 (2014).

8) Sixta, H., Michud, A., Hauru, L., Asaadi, S., Ma, Y. and King, A., Kilpeläinen, I., and Hummel, M.: Cellulose dissolution and regeneration: systems and interactions. Nordic Pulp & Paper Research Journal Vol 30 no (1), 49-57 (2015).

9) Franz, M. H.: The cellulose gap (the future of cellulose fibers), Lenz. Ber. 89, 12-21 (2011).

10) Matsunaga, T. and Ikada, Y.: Surface modifications of cellulose and polyvinyl alcohol, and determination of the surface density of the hydroxyl group. In, Modification of Polymers, ACS Symposium Series, Vol. 121, Chapter 26, 391-406 (1980).

11) Lindman, B., Karlström, G. and Stigsson, L.: On the mechanism of dissolution of cellulose, Journal of Molecular Liquids, 156, 76–81 (2010).

12) Medronho, B. and Lindman, B.: Competing forces during cellulose dissolution: From solvents to mechanisms, Current Opinion in Colloid & Interface Science, 19, 32-40 (2014).

13) Medronho, B., Romano, A., Miguel, M. G., Stigsson, L. and Lindman, B.: Rationalizing cellulose (in) solubility: re-viewing basic physicochemical aspects and role of hydrophobic interactions, Cellulose, 19, 581–587 (2012).

14) Yamane, C., Aoyagi, T., Sato, K., Okajima, K. and Takahashi, T.: Two different surface properties of regenerated cellulose resulting from structural anisotropy. Polymer Journal, 38, 819-826 (2006).

15) Hongo, T., Koizumi, T., Yamane, C. and Okajima, K.: Thermally Stimulated Depolarized Current (TSDC) Analysis on the Structural Change of Regenerated Cellulose Membranes Caused by the Change in Water Content, Polymer Journal, 28, 1077-1083 (1996)

16) Hongo, T., Yamane, C., Saito, M. and Okajima, K.: Super-Molecular Structures Controlling the Swelling Behavior of Regenerated Cellulose Membranes, Polymer Journal, 28(9), 769-779 (1996).

17) Miyamoto, H., Umemura, M., Yamane, C., Ueda, K. & Takahashi, T.: Structural reorganization of molecular sheets derived from cellulose II by molecular dynamics simulations. Carbohydrate Research, 344, 1085-1094 (2009).

18) Isobe, N., Kimura, S., Wada, M. and Kuga, S.: Mechanism of cellulose gelation from aqueous alkali-urea solution. Carbohydrate Polymers, 89(4), 1298-1300 (2012).

19) Yamane, C., Hirase, R., Miyamoto, H., Kuwamoto, S. and Yuguchi, Y.: Mechanism of structure formation and dissolution of regenerated cellulose from cellulose/aqueous sodium hydroxide solution and formation of molecular sheets deduced from the mechanism. Cellulose, 22(5), 2971-2982 (2015).

20) Yamane, C.: Structure formation of regenerated cellulose from its solution and

resultant features of high wettability: A review, Nordic Pulp and Paper Research Journal Vol 30(1), 78-91 (2015).

21) Hayashi, J., Matuda, S. and Watanabe, S.: Plane lattice structure in amorphous region of cellulose fibers. Nippon Kagaku Kaishi, 5, 948-954 (1974).

22) Hermans, P. H. and Weidinger, A.: Quantitative X-Ray Investigations on the Crystallinity of Cellulose Fibers. A Background Analysis. Journal of Applied Physics, 19, 491–506 (1948).

23) Hermans, P. H.: Degree of lateral order in various rayons as deduced from x-ray measurements. Journal of Polymer Science, 4(2), 145–151 (1949).

24) Yamane, C., Mori, M., Saito, M. and Okajima, K.: Structure and Mechanical Properties of Cellulose Filament Spun from Cellulose/aq. NaOH Solution, Polymer Journal, 28(12), 1039-1047 (1996).

25) Takizawa, T., Kawaguchi H. and Nagura, T.: Development of the cotton 100% Non-Iron shirt, Jpn. Res. Assn. Text. 57(11), 834-837 (2016).

26) Ito, T.: New Technology in Textile Processing “J-Wash”. Journal of the Textile Machinery Society of Japan 52(10), 422-426 (1999).

27) Okajima, S., Inoue, K. and Yazawa M.: Studies on lowering of the degree of swelling of rayon, Sen'i Gakkaishi, 18, 9, 807-813 (1962).

Chapter 2. Relaxation phenomenon and swelling behavior of regenerated cellulose fibers affected by water

2.1. Introduction

Cellulose precipitated from cellulose solution by non-solvents is classified as regenerated cellulose and is used in many fields such as textile fibers, cellophane films, cellulose sponges and meat casings. The commercially available regenerated cellulose fibers are rayon, cupra and lyocell, and prepared from each cellulose solution of CS_2/aqueous NaOH, Cu/aqueous NH_3 and *N*-methyl morpholine *N*-oxide (NMMO), respectively. Research and development of rayon and cupra have long history started from the late nineteenth century. The discovery of NMMO as strong cellulose solvent was the starting point of the development of lyocell fiber[1)], and then commercial production of lyocell as the trade name of TENCELL™ has been started from the late twentieth century. Inclusive review of NMMO system was written by Fink, Ganster, & Lehmann[2)]. Lyocell process will gradually become major production system of regenerated cellulose fibers instead of rayon process due to its environmentally friendly process with a closed system. Many production systems have been investigated in order to propose next-generation fibers such as "BioCelsol" prepared from aqueous NaOH solution system incorporated with enzyme treatment (for example, Budtova & Navard[3)], "CarbaCell" from NaOH/urea in o-xylene[4)], "BoCell" from anisotropic solutions of cellulose in phosphoric acid and spun via air-gap into acetone[5, 6)], and "Ioncell-F" from cellulose solution in ionic liquid (1,5-diazabicyclo [4.3.0] non-5-enium acetate) and spun via air-gap into coagulants[7, 8)]. These studies mainly focused on practical properties for textile use such as tensile strength, elongation and Young's modulus, and general structural parameters obtained by wide angle X-ray, ^{13}C-NMR and electron microscopes. Nevertheless, it remains unclear what kind of properties and structure should be required for next-generation fibers.

Regenerated cellulose is one of the most hydrophilic polymers, having an extremely wettable surface. The contact angles of water droplets on cellophane and cuprophane,

which are typical regenerated cellulose films, were shown to be 11.6º and 12.2º, respectively. These angles are far lower than those of widely-used polymers. Although the hydrophilic polymer poly (vinyl alcohol) (PVA), which contains many hydroxyls, has a low contact angle (36º), this value is still higher than those of regenerated cellulose films. It is notable that the contact angle of water on starch film is 41º. The high wettability of regenerated cellulose films could be attributed to the higher density of hydroxyl groups on a cellulose surface than on a PVA surface; the densities of hydroxyls on the film surfaces of cellophane and PVA were 1×10^{-5} and 5×10^{-6} mol m^{-2}, respectively[9]. The $(1\bar{1}0)$ crystal plane of cellulose II polymorph lies parallel to the surface of regenerated cellulose (uni-planar orientation of $(1\bar{1}0)$ plane), and the density of hydroxyls on the crystal plane is geometrically high due to their equatorial connection to glucopyranose[10, 11]. During the regeneration process from cellulose solution leading to deliberately-shaped regenerated cellulose, hydrophobic interaction among –C-H residues on the glucose plane stacks cellulose molecules to form a thin planar structure with many hydroxyls on its surface[12]. This is the basic structure of regenerated cellulose, and brings about high wettability[13]. These structures with many hydroxyls are piled together in an orderly way by hydrogen bonds to form crystals, some of which irregularly aggregate and/or remain as they are, forming amorphous regions. The amorphous regions thus formed with many accessible hydroxyls, i.e., with large areas of hydrophilic inner surfaces, can absorb considerable amounts of water. The swelling ratio is defined as the ratio of the weight/weight percentage (w/w %) of water that remains in fibers after centrifugation at 1,000 × *g*, to dry weight. The range of the swelling ratio of regenerated cellulose is 50-200%. The water could loosen interactions among cellulose molecules, decreasing the density of the permeating area and making a space in the amorphous region. It is possible that (1) water penetration into the amorphous causes segmental movement of cellulose molecules such as micro-Brownian motion of main chains, and (2) the swelling due to water widening the space in the amorphous region is related to the relaxation phenomenon of regenerated cellulose.

Water markedly lowers the wet moduli of regenerated cellulose. The ratios of

wet/conditioned moduli were 1/24, 1/6, and 1/13 for rayon, cupra and lyocell, respectively[14], suggesting that some segmental movements in cellulose main chains are released in the wet state. When fabrics made of regenerated cellulose fibers such as rayon, cupra and lyocell are washed with water, wrinkling, shrinking and fibrillation occur, which usually requires them to be dry-cleaned. To understand these issues, the dynamic viscoelastic behavior caused by water and the relating swelling phenomenon should be clarified.

2.2. Materials and Methods

2.2.1. Materials

Three kinds of regenerated cellulose fibers were used: viscose rayon, rayon (1.7 dtex, Omikenshi Co., Ltd.); cuprammonium rayon filaments, cupra (110 dtex/ 60 filaments, Asahi Kasei Co., Ltd.) and solvent spun rayon, lyocell (1.7 dtex, Lenzing AG). The unit of dtex (deci-tex) is a direct measure of linear density: dtex; grams per 10 kilometers of yarn and fibers.

2.2.2. Dynamic Viscoelasticity

The effect of water regains on the storage modulus (*Er*) and the mechanical loss tangent δ (the ratio of *Er* to loss modulus of the fibers, tan δ) were evaluated using a viscoelastic spectrometer (DVA-200, IT Keisoku Seigyo Co., Ltd., Japan) under the following conditions: frequency, 10 Hz; temperature, 298 K; and sample length, 20 mm. The sample was immersed in water for 10 min and extra water was removed, then the wet fiber bundle was cut into two halves of the same weight. One half was used for viscoelastic measurement. The apparatus was placed in a conditioned room (298 K and 65% RH) and the measuring samples were not sealed to contact with atmospheric air. The other half was simultaneously placed close to the measuring spot and the weight was measured every 30 seconds to determine the time-dependence of water regain, and then the time–tan δ curve was changed to a water regain–tan δ curve.

2.2.3. Tensile strength and elongation

The bundle of regenerated cellulose filaments (lyocell) was immersed in water for 10 min and dried so as to obtain the respective water regain, and the measurements were carried out in a conditioned room (298 K and 65% RH) under the following conditions and apparatus: initial clamp separation, 100 mm; elongation speed, 100 mm/min; apparatus, FGS-50E, Shimpo Co., Ltd, Japan. Just after each measurement, the sample was weighed to precisely determine the water regain.

2.2.4. Wide angle X-ray scattering (WAXS)

X-Ray diffraction patterns of regenerated cellulose fibers were measured by a reflection method and recorded on X-ray diffraction apparatus (RINT2000, Rigaku Co., Ltd., Japan). The sample fibers (rayon, cupra, lyocell) were cut into particle-like sizes less than ca. 120 μm to negate the influence of crystalline orientation, and recorded on the X-ray diffractometer equipped with a scintillation counter under the following conditions: wavelength, 0.154 nm; acceleration voltage and current, 40 kV and 40 mA; and scattering angle, 2 θ = 5-30°. The crystallinity index (*Xc*) was estimated by peak areas responsible for the ($1\bar{1}0$), (110) and (020) planes, separated by the Lorents-Gaussian peak separation method. Apparent crystal size (ACS) was estimated by the Scherrer's *Eq* 1[15]:

$$ACS = (\kappa\lambda/\cos\theta)/\mu \qquad (1)$$

$$\mu = (B^2-b^2)^{1/2} \qquad (2)$$

where κ is an apparatus constant taken as 0.9: λ, wavelength of the Cu Kα line (0.1542 nm); θ, Bragg angle; B, angular width in radians corresponding to the half-intensity width of the diffraction peaks; and b, another apparatus constant (0.0035 in radians).

2.2.5. Small angle X-ray scattering (SAXS)

In order to investigate the periodicity of the intervals of microfibrils accompanying swelling of regenerated cellulose fibers, small angle two-dimensional scattering images were obtained by high intensity X-ray synchrotron radiation. The bottom of a glass capillary purchased from WSJ-Glas, Müller GmbH, Germany, was broken to make a glass tube. A bundle of fibers was slipped into the glass tube (diameter 3.0 mm, length 80 mm, thickness 0.01 mm), a specific amount of water was added into the glass tube using a micro-syringe to adjust the water regains to the respective values, and the upper and lower ends of the tube were sealed with glue to prevent water evaporation. After the water was uniformly dispersed in the fiber bundle, SAXS measurements were conducted at the experimental station of BL-40B in the synchrotron radiation facility, SPring-8, located in

Hyogo prefecture, Japan. The wavelength of the incident X-ray was adjusted to 0.1 nm; camera length was 1206.4 mm; irradiation time was 1.0 sec; and the X-ray beam was focused to a point. The intensity of SAXS was detected by imaging plate. The resulting two-dimensional scattering images were scanned on the equator line, and the long periods were estimated from the positions (q: the scattering vector) of the peaks and shoulders observed.

2.3. Results and Discussion

2.3.1. Relaxation phenomenon of regenerated cellulose fibers

The temperature dependence of dynamic viscoelasticity should first be known in order to study the relaxation behavior of regenerated cellulose fibers caused by water. The temperature dependence of tan δ for the fibers has been previously examined as shown in Figure 2-1[14].

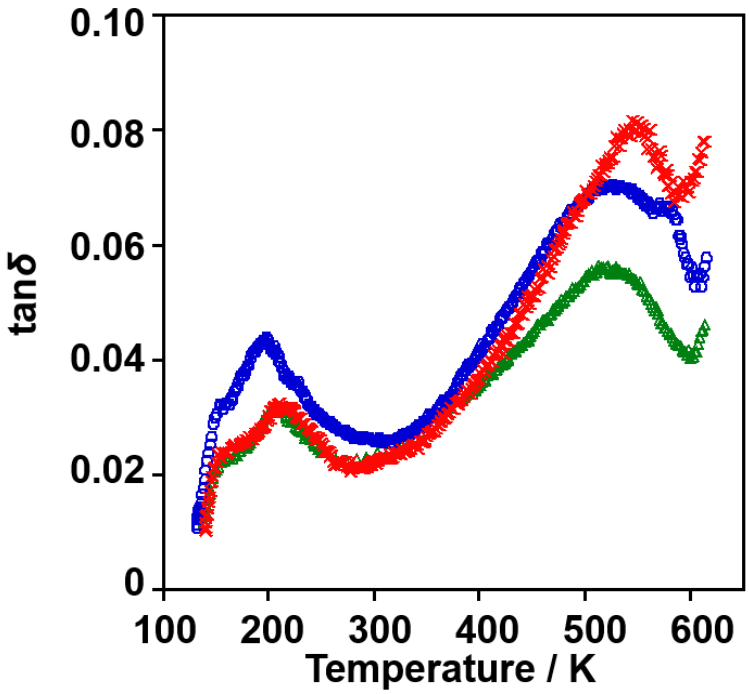

Figure 2-1. Temperature dependence of tan δ for regenerated cellulose fibers: ×, rayon (2.5 dtex, Asahi Kasei Co., Ltd., Japan); ○, cupra (83 dtex/ 45 filaments, Asahi Kasei Co., Ltd., Japan); △, lyocell (1.7 dtex, Lenzing AG, Austria). Reproduced from (Yamane et al. 1996) with permission of The Society of Polymer Science, Japan.

The peaks of tan δ were observed at low temperatures from 190 K to 210 K and at high temperatures from 510 K to 550 K for all fibers. It was reported that the peaks of the low and high temperature regions were assigned to the local segmental motion of cellulose molecules and the micro-Brownian motion of cellulose main chains in amorphous regions,

respectively[14, 16]. The temperatures of the peaks (T_{max}) in the high temperature region are related to the glass transition temperature. Here, the peak temperatures (T_{max}) and peak heights (tan δ_{max}) were aligned: the T_{max} values were 552 K for rayon, 523 K for cupra and 513 K for lyocell in order of temperature; and the tan δ_{max} values were 0.082 for rayon, 0.070 for cupra and 0.056 for lyocell in order of peak height (Table 2-1).

Table 2-1. Transition of regenerated cellulose fibers and the saturated water regain

	Thermal transition		Water transition		Saturated water
	T_{max}/K	Tan δ_{max}	WR_{max}/%	Tan δ_{max}	regain /%[*1]
Rayon	552[*2]	0.082[*2]	78 (± 0.8)	0.22 (± 0.02)	47 (± 0.7)
Cupra	523[*2]	0.070[*2]	63 (± 0.5)	0.14 (± 0.01)	37 (± 1.2)
Lyocell	513[*2]	0.056[*2]	56 (± 1.8)	0.11 (± 0.01)	31 (± 0.7)

*1 Water regain at temperature 298 K and relative humidity 100%. *2 Cited from (Yamane et al. 1996[14]). Three replications were applied to the measurements of dynamic viscoelasticity and saturated water regains, and standard deviations are listed in parenthesis.

In general, T_{max} is governed by the segmental environment such as packing regularity and intermolecular forces in the amorphous region, and tan δ_{max} qualitatively indicates the size of the moving unit. Although rayon has the largest moving unit (the highest tan δ_{max}), its packing regularity and/or intermolecular forces are the highest (the highest T_{max}), and lyocell is quite the reverse with the lowest tan δ_{max} and T_{max}. Lyocell had the highest crystallinity index (*Xc*) listed in the former report[14]. The highest *Xc* indicated the smallest volume of amorphous region which resulted in the lowest tan δ_{max} and the smallest moving unit. The reason of the lowest T_{max} of lyocell has been explained that "crystallization might exclude some strains to microcrystalline interval" and "the strains excluded into amorphous region makes molecular order more random when *Xc* is larger, leading to lower shift of T_{max}" [14]. In this study, we investigated the effect of water on viscoelastic phenomena for regenerated cellulose fibers based on the studies of thermal relaxation mentioned above.

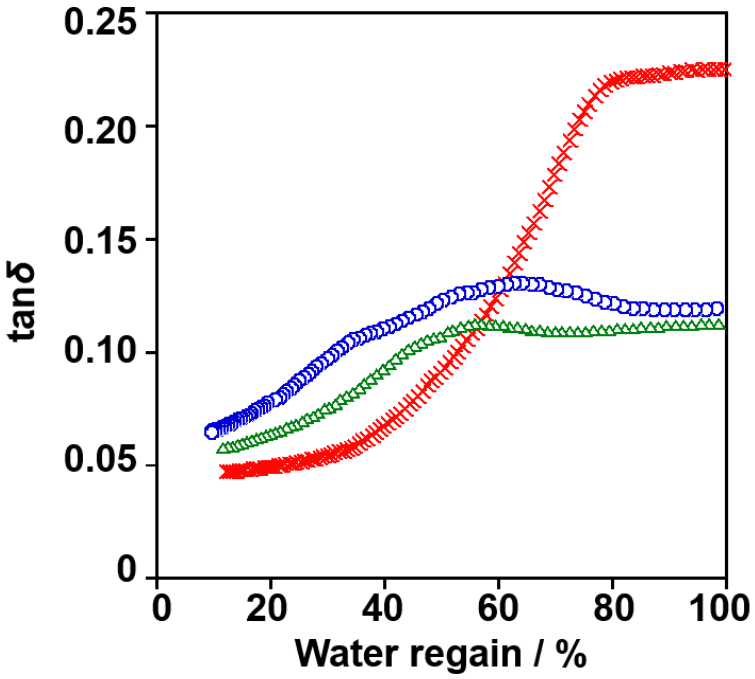

Figure 2-2. Relationship between water regain of regenerated cellulose fibers and viscoelastic parameter tan δ at 298 K: ×; rayon, ○; cupra, △; lyocell.

The water regain is expressed as the weight/weight percentage (w/w%) of water in a fiber versus the fiber's dry weight. When the water regains of the fibers were changed during the measurements, peaks and shoulder of tan δ were observed (Figure 2-2) similar to their appearance in the measurements of temperature dependence. The fibers used in this study were not the same but similar to those previously used for the measurements of temperature dependence shown in Figure 2-1. The maximum of tan δ is associated with molecular movement and/or some transitions as quoted from books: "the tan δ peak is associated with the partial loosening of the polymer structure so that groups and small chain segments can move. This occurs near glass transition temperature at low frequencies"[17] and "in the transition zone between glasslike and rubberlike consistency, tan δ goes through a maximum for both uncross-linked polymers of high molecular weight and lightly cross-linked polymers"[18]. Accordingly, the peaks and shoulder must be caused by molecular movement and/or some transitions in the amorphous regions. The water

regains of the peaks and shoulder (WR_{max}) were 78% for rayon, 63% for cupra, and 56% for lyocell. Rayon needed the largest amount of water to cause the transition at room temperature, followed by cupra and lyocell. The crystallinity index (*Xc*) was in the order of 35.4% for lyocell, 34.4% for cupra, and 31.4% for rayon. This suggests that the amorphous region of rayon is the largest, which is consistent with rayon requiring the highest amount of water to cause the molecular motion of main chains in the amorphous region. On the other side, the glass transition temperatures indicated by T_{max} were higher in the order of rayon, cupra and lyocell, as listed in Table 2-1; the highest T_{max} and WR_{max} for rayon suggested that rayon could have a well-ordered and tightly packed amorphous region as well as a large size of moving unit. This trend became weaker for cupra, followed by lyocell. The values of tan δ_{max} caused by water were in the order of 0.22 for rayon, 0.14 for cupra and 0.11 for lyocell, which was the same order as for tan δ_{max} caused by thermal transition: 0.082 for rayon, 0.070 for cupra and 0.056 for lyocell (Table 2-1). The difference in tan δ_{max} between the water transition and the thermal transition was its absolute value; the values of water transition were 2.0-2.7 times that of tan δ_{max} of the corresponding thermal transition. This indicates that the volume of the structural region affected by water could be much larger than that affected by temperature. We concluded that the relaxation peaks including the shoulder caused by water and high temperature had similar trends among regenerated cellulose fibers except for the absolute value of tan δ_{max}.

Cellulose derivatives which have three and two acetyl groups in each pyranose are tri-acetate and di-acetate, respectively. Although acetate is classified as cellulose-derived fiber, it is used in a similar way to regenerated cellulose fibers. Effect of water regain of acetate fibers on tan δ at 298 K was measured and peaks of tan δ were observed. We used tri-acetate (84 dtex/ 20 filaments, Mitsubishi Rayon Co., Ltd., Japan) and di-acetate (84 dtex/ 20 filaments, Mitsubishi Rayon Co., Ltd., Japan). WR_{max} were 55% and 51% for tri-acetate and di-acetate, respectively. Water would cause molecular movement and/or some transitions of acetate like regenerated fibers. Tan δ_{max} of acetate were 0.055 and 0.051 for tri-acetate and di-acetate, which were far lower than those of regenerated cellulose fibers;

0.22, 0.14 and 0.11 for rayon, cupra and lyocell, respectively. A probable size of moving unit of acetate affected by water would be smaller than those of regenerated cellulose fibers.

The storage modulus *Er* decreased sharply with increasing water regain until the regain reached WR_{max}, and then levelled off; the values for rayon, cupra and lyocell were 1/10, 1/8 and 1/3, respectively, compared to their starting values (Figure 2-3).

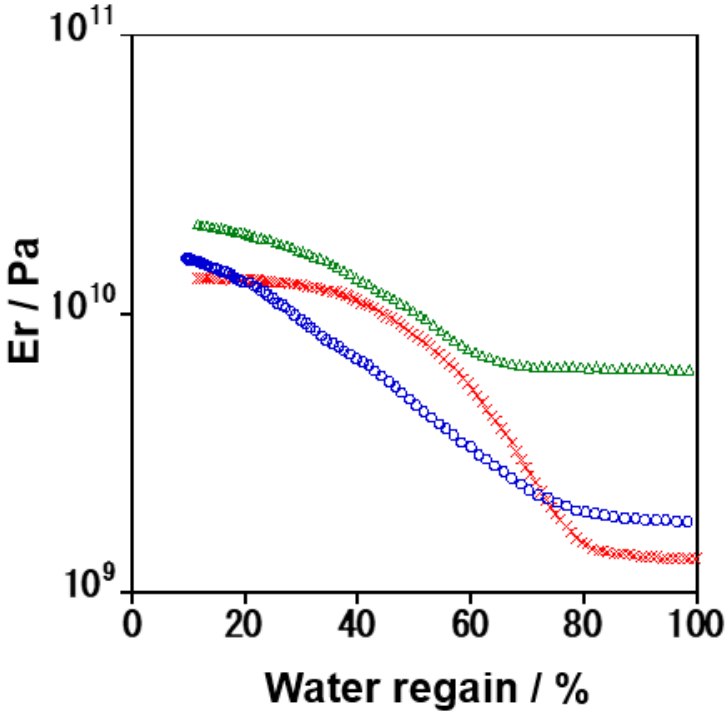

Figure 2-3. Relationship between water regain of regenerated cellulose fibers and storage elastic modulus *Er* at 298 K; ×, rayon; ○, cupra; △, lyocell.

This sharp decrease of *Er* is observed in the glass transitions of many thermoplastic polymers. The similarity of tan δ, specifically that of temperature dependency and water regain dependency of tan δ among regenerated cellulose fibers, and the sharp decrease of *Er* at near WR_{max}, indicate that the specific water regains (WR_{max}) probably cause glass transitions at room temperature for regenerated cellulose fibers. Even in the amorphous region, a portion of cellulose chains builds up to large extent intra- and intermolecular

hydrogen bonds, which may make the occurrence of the micro-Brownian motion difficult at low temperatures. It is reasonable to suppose that water can penetrate into the amorphous region, loosening the bonds and widening the region, and in consequence the glass transition temperature decreases from 510 - 550 K to room temperature. Thus, the regenerated cellulose fibers change from glassy state to so-called rubbery state at water regains of 78% (rayon), 63% (cupra) and 56% (lyocell) at 298 K. It is known that the glass transition temperature decreases by the addition of a diluent (plasticizer) expressed by the Fox equation (3)[19]:

$$\frac{1}{T_g} = \frac{w_1}{T_{g1}} + \frac{(1-w_1)}{T_g^0} \qquad (3),$$

where T_g is the glass transition temperature of polymer with a diluent, w_1 is the weight fraction of a diluent, T_{g1} is the glass transition temperature of a diluent and T_g^0 is the glass transition temperature of polymer without a diluent. When a diluent does not have the glass transition temperature, T_{g1} works as an imaginable constant. In general, a diluent is low molecular weight molecules and has lower T_{g1} than T_g^0, resulting in lower T_g than T_g^0 calculated from equation (3). For instance, the glass transition temperature of poly (vinyl chloride) decreased by 70 °C plasticized with succinate esters[20]; water decreased the glass transition temperature of microcrystalline cellulose powder detected by differential scanning calorimetry[21].

Figure 2-4 shows Stress-Strain (S-S) curves of lyocell with various water regains. The initial modulus (Young's modulus) and the strength decreased, and the elongation increased with increasing water regain. In particular, Young's modulus significantly decreased until the water regain reached 40%, and appeared to be leveled off near the WR_{max} (56%). This also suggests that lyocell changes to the rubbery state at a water regain above the WR_{max}. The transition from glassy to rubbery state is understandable from daily experience; for example, cellulose sponge, which is regenerated cellulose made from viscose rayon solution, changes from hard when dry to soft when wet. The transition also causes problems for textile use; dry cleaning is generally applied to fabrics made of

regenerated cellulose fibers to avoid significant wrinkling by home-washing. Crumpling and rubbing by a washing machine in water, where regenerated cellulose becomes rubbery, followed by drying into the glassy state, could be the main reason for deep wrinkles during home-washing. Polyester fabric is washable, but if it were washed in conditions above the glass transition temperature, followed by cooling, it would have similar wrinkles to regenerated cellulose fabric. The water regains at a room temperature of 298 K and relative humidity of 100% (hereinafter referred to as saturated water regain) were 47% for rayon, 37% for cupra, and 31% for lyocell. This indicates that the water regain of regenerated cellulose cannot reach WR_{max} even in high humidity conditions in daily life. Adding a small amount of water puts regenerated cellulose into the rubbery state. Zhou et al.[22] conducted a dynamic mechanical analysis of the effects of water uptake on regenerated cellulose; however, they could not find micro-Brownian movement of cellulose main chains because the range of water regain tested was limited to 0-40%.

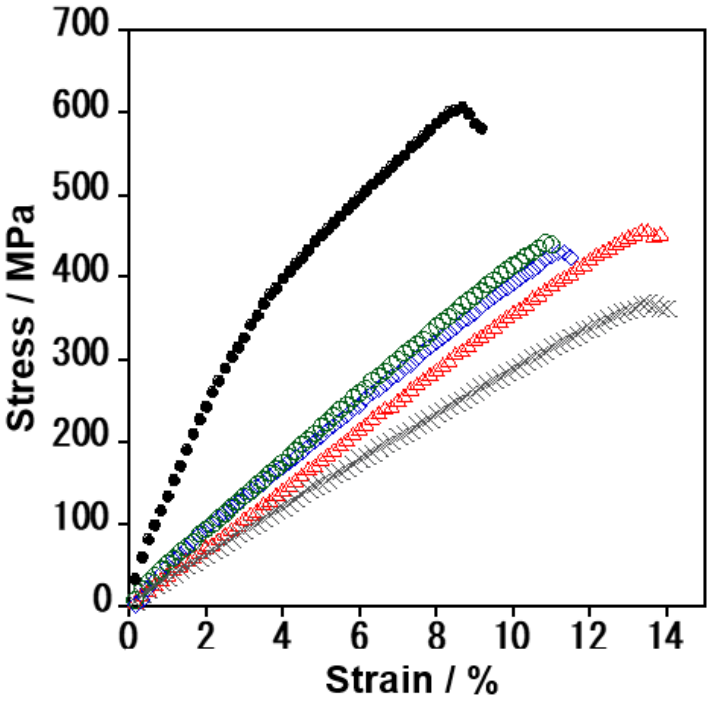

Figure 2-4. Stress-strain curves of regenerated cellulose fibers (lyocell) with various water regains: ●, 9%; ○, 33%; ◇, 37%; △, 60%; ×, 65%.

2.3.2. Swelling behavior of regenerated cellulose fibers

Small-angle X-ray scattering images of regenerated cellulose fibers (lyocell) with various water regains are shown in Figure 2-5.

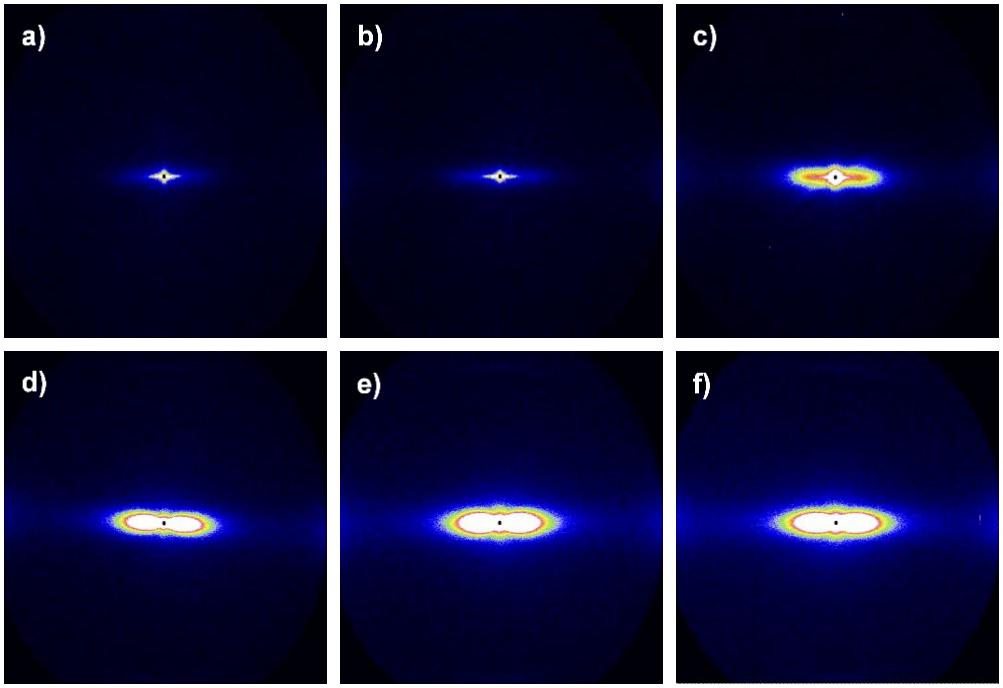

Figure 2-5. Small angle scattering images of regenerated cellulose fiber (lyocell) with various water regains: a), 0%; b), 9%; c), 30%; d), 50%; e), 75%; f), 100%.

Here, the bundles of fibers were placed vertically. The equatorial intensity at water regains of 0% and 9% appeared to decrease monotonically toward the wide-angle side. As the water regains increased, the overall intensity increased, and there seemed to be a maximum at over 30% water regains. Indeed, when the intensity was scanned along the equatorial line, scattering peaks and shoulders were observed (Figure 2-6). These peaks and shoulders became more pronounced with increasing water regains, and shifted to the low angle side. Similar scattering profiles were observed for rayon and cupra (figures not shown), except that rayon with 0% water regain and cupra with 0% and 9% water regains had no peaks or shoulders, i.e., the scattering profiles along the equatorial line decreased monotonically.

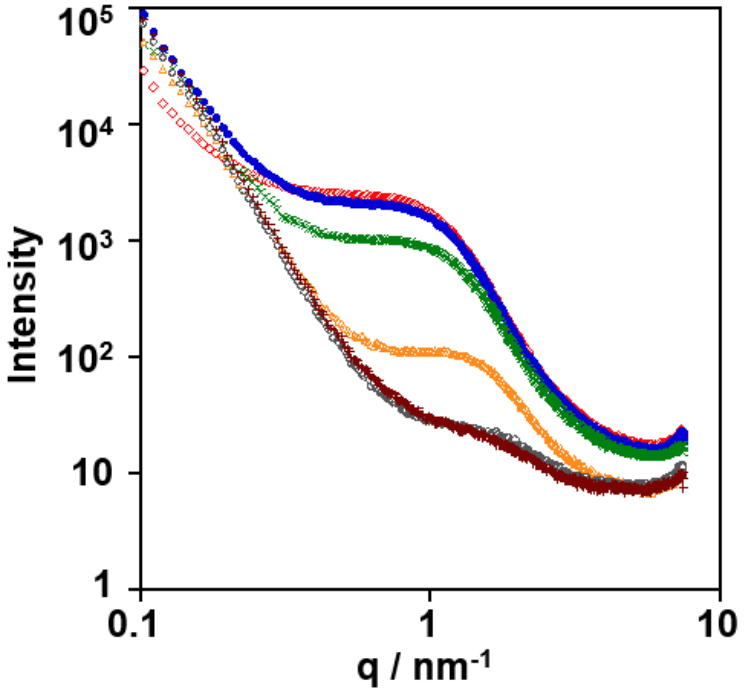

Figure 2-6. Small angle scattering profiles on the equator line of regenerated cellulose fiber (lyocell) with various water regains: ◇, 100%; ●, 75%; ×, 50%; △, 30%; ○, 9%; +, 0%.

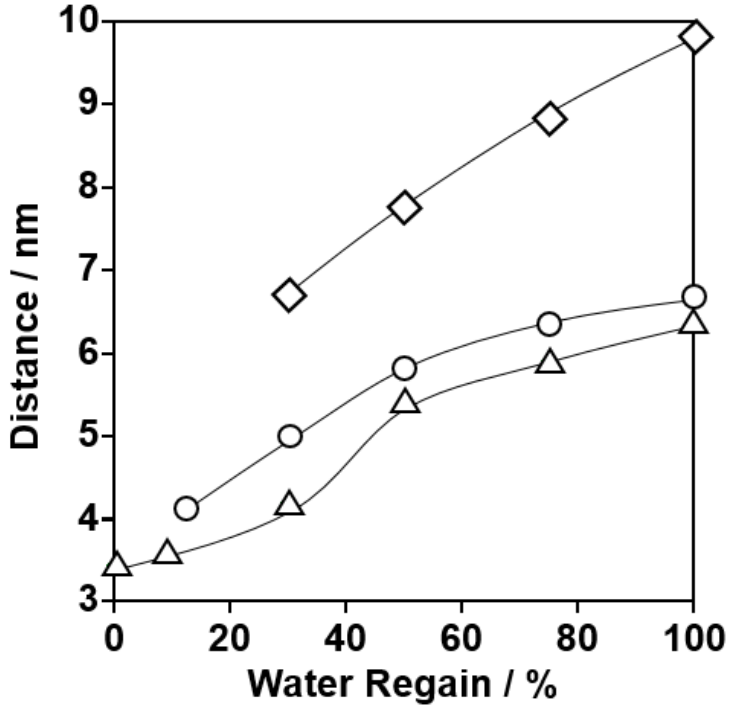

Figure 2-7. Long periods of regenerated cellulose fibers with various water regains: ○, rayon; ◇, cupra; △, lyocell.

Figure 2-7 shows the long periods estimated from the scattering vector *q* of these peaks and shoulders. There were no data plots at 0% for rayon or 0% and 9% for cupra, due to the absence of scattering peaks or shoulders. The long periods extended with increasing water regain in all regenerated cellulose fibers. The long periods of rayon and lyocell seemed to be leveled off for water regains higher than WR_{max}. This corresponded to the changes in *Er* and Young's modulus estimated from S-S curves shown in Figure 2-3 and 2-4, which also leveled-off in the same region of water regain. These results suggested that the changes in long periods caused by water could be related to the relaxation phenomenon. The long period of lyocell was 3.4 nm at 0% water regain. Extrapolation of the long periods of rayon and cupra to the water regain of 0% resulted in about 3.6 and 4.5 nm, respectively. The apparent crystal sizes (ACS) of the regenerated cellulose fibers were estimated by Scheller's equation[15]. The ACS of (110), (020) and ($1\bar{1}0$) were 3.98, 3.99 and 3.94 nm for rayon; 3.50, 3.84 and 3.99 nm for cupra; and 3.67, 3.52 and 3.64 nm for lyocell, respectively. Although the long periods of cupra were slightly larger, the long periods in the dry state were similar to the ACS. Therefore, these long periods could be related to the distances among microcrystals, which are the component of microfibrils. The microfibrils of regenerated cellulose fibers have been defined by Yachi, Hayashi, Takai, & Shimizu[23] as trains of microcrystals with a width of 3.5 nm and length of 20 nm, connected with each other along the *c* axis direction. In the case of natural cellulose, microfibrils with a width of about 4 nm and also appearing as trains of microcrystals are observed by transmission electron microscopy[24]. Regenerated cellulose fibers are likely also composed of microfibrils having almost the same width as that of natural cellulose. Moreover, bundles of microfibrils about 30 nm wide have been observed in cupra[25]. Therefore, the appearance of these scattering peaks or shoulders could be caused by differences in electron density between crystals (density of cellulose II, 1.60 g/cm^3: Langan et al.[26]) and inter-crystalline regions where water easily penetrates and reduces the density, and the long period could be the distance between microfibrils, which is schematically depicted in Figure 2-8. SAXS and small-angle neutron scattering (SANS)

study of wood with various water regain concluded that SAXS and SANS profiles showed the packing distance of cellulose microfibrils[27], which supports our discussions.

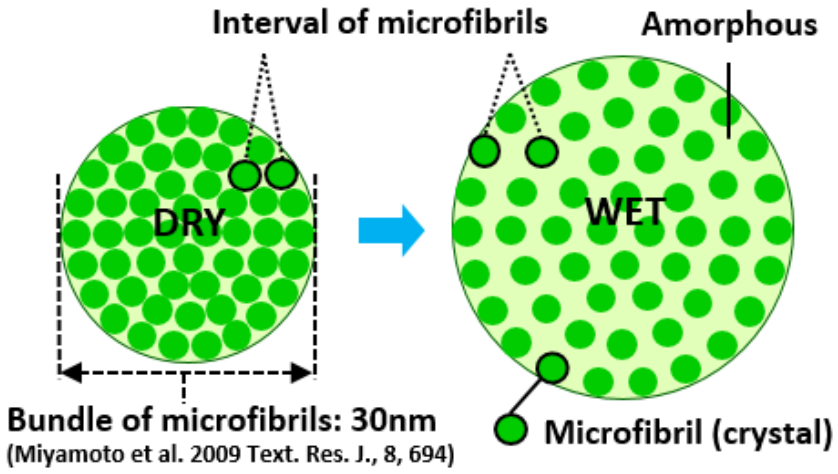

Figure 2-8. Schematic diagram of bundle of microfibrils and change in interval of microfibrils by wetting.

The shoulders of lyocell with 0% and 9% water regains were extremely small (Figure 2-6), and no peaks or shoulders were observed for 0% water regain of rayon and 0 and 9% water regains of cupra. This suggests that there is almost no difference between the density of microfibrils and that of inter-microfibrils in the dry state. Indeed, Hermans et al.[28, 29] reported that the density of amorphous regions of regenerated cellulose was slightly lower, by only 6%, than that of crystals. As mentioned above, T_{max} qualitatively expresses the segmental environment such as packing regularity and intermolecular forces in the amorphous region, and T_{max} of lyocell was the lowest; therefore, lyocell might have a lower density than those of rayon and cupra, resulting in the appearance of the small shoulder at 0% of water regain, while no shoulders were observed for rayon or cupra in the same conditions.

To summarize the changes in physical properties and structures caused by water: First, water penetrates into the dry space among microfibrils to lower the *Er* and Young's modulus and widen that region. Subsequently, the water regain reaches saturated water regain (rayon, 47%; cupra, 37%; lyocell, 31% listed in Table 2-1). However, overall molecular movement of the cellulose backbone has not yet occurred at this stage. When water further infiltrates into the regions; changes in *Er*, Young's modulus and the distance between microfibrils are leveled off; and the water regain reaches WR_{max} (rayon, 78%; cupra, 63%; lyocell, 56%) where the peaks or shoulder of tan δ appear. In this state, the main chain of the cellulose molecule starts to move and the regenerated cellulose fibers change to a so-called rubbery state. The transition might require sufficient space for movement of cellulose main chains. The result that tan δ_{max} caused by water was 2.0-2.7 times larger than that caused by thermal transition corresponds to this space for molecular movement.

2.4. Conclusions

Tan δ peaks and shoulder were observed in tan δ-water regain curves at WR_{max}; 78% for rayon, 63% for cupra and 56% for lyocell at room temperature. *Er* markedly decreased around these water regains. It is possible that the mechanical absorption is due to micro-Brownian movement of the cellulose main chains; in other words, the glass transition temperatures of 510-550 K of regenerated cellulose fibers would shift to room temperature at specific water regains. Even in the amorphous region, a portion of cellulose chains builds up to large extent intra- and intermolecular hydrogen bonds, which may make the occurrence of micro-Brownian motion difficult at low temperature. Water probably loosened the hydrogen bonds and widened the space of the amorphous region, resulting in the marked decrease in glass transition temperature. The order of tan δ_{max} among the fibers was the same as that of WR_{max}; 0.22 for rayon, 0.13 for cupra and 0.11 for lyocell, indicating that rayon would have the largest size of moving unit, followed by cupra and lyocell. The tan δ_{max} values observed in the thermal transitions were extremely low compared to the water transitions; 0.082 for rayon, 0.072 for cupra and 0.056 for lyocell. This also indicates that water increased the volume of moving units by loosening intermolecular forces and widening the space between cellulose molecules. SAXS showed the maxima and shoulders on the equator line in the wet state, suggesting that water decreased the density of the amorphous region, i.e., widened the space between cellulose molecules, creating sufficient space for the micro-Brownian motion of cellulose main chains.

References

1) Johnson, D. L.: Process for strengthening swellable fibrous material with an amine oxide and the resulting material, Eastman Kodak Company, US patent 3447956 (1969).

2) Fink, H. P., Ganster, J., & Lehmann, A.: Progress in cellulose shaping: 20 years industrial case studies at Fraunhofer IAP. Cellulose, 21, 31-51 (2014).

3) Budtova, T., & Navard, P.: Cellulose in NaOH–water based solvents. Cellulose, 23(1), 5-55 (2016).

4) Wendler, F., Schulze, T., Ciechanska, D., Wesolowska, E., Wawro, D., Meister, F., Budtova, T., & Liebner, F.: Cellulose products from solutions: film, fibers and aerogels; The European Polysaccharide Network of Excellence (EPNOE); Springer: Vienna, 153− 185 (2013).

5) Northolt, M.G., Boerstoel, H., Maatman., Huisman, R., Veurink, J., & Elzerman, H.: The structure and properties of cellulose fibers spum from an anisotropic phosphoric acid solution. Polymer, 42, 8249-8264 (2001).

6) Röder, T., Moosbauer, J., Wöss, K., Schlader, S., & Kraft, G.: Man-made cellulose fibres – a comparison based on morphology and mechanical properties. Lenzinger Berichte, 91, 7-12 (2013).

7) Michud, A., Tanttu, M., Asaadi, S., Ma, Y., Netti, E., Kääriäinen, P., Persson, A., Berntsson, A., Hummel, M., & Sixta, H.: Ioncell-F: ionic liquid-based cellulosic textile fibers as an alternative to viscose and Lyocell. Textile Research Journal, 86 (5), 543-552 (2016).

8) Sixta, H., Michud, A., Hauru, L., Asaadi, S., Ma, Y., King, A. W. T., Kilpelainen I., & Hummel M.: Ioncell-F: a high-strength regenerated cellulose fiber. Nordic pulp & paper research journal, 30(1), 43-57 (2015).

9) Matsunaga, T., & Ikada, Y.: Surface modifications of cellulose and polyvinyl alcohol, and determination of the surface density of the hydroxyl group. In, Modification of Polymers, ACS Symposium Series, Vol. 121, Chapter 26, 391-406 (1980).

10) Miyamoto, H., Umemura, M., Yamane, C., Ueda, K., & Takahashi, T.: Structural

reorganization of molecular sheets derived from cellulose II by molecular dynamics simulations. Carbohydrate Research, 344, 1085-1094 (2009).

11) Yamane, C., Aoyagi, T., Sato, K., Okajima, K., & Takahashi, T.: Two different surface properties of regenerated cellulose resulting from structural anisotropy. Polymer Journal, 38, 819-826 (2006).

12) Isobe, N., Kimura, S., Wada, M., & Kuga, S.: Mechanism of cellulose gelation from aqueous alkali-urea solution. Carbohydrate Polymers, 89, 1298-1300 (2012).

13) Yamane, C.: Structure formation of regenerated cellulose from its solution and resultant features of high wettability. Nordic Pulp and Paper Research Journal, 30, 78-91 (2015).

14) Yamane, C., Mori, M., Saito, M., & Okajima, K.: Structures and mechanical properties of cellulose filament spun from cellulose/aqueous NaOH solution system. Polymer Journal, 28, 1039-1047 (1996).

15) Scherrer, P.: Determination of the size and internal structure of colloidal particles using X-rays. Nachr. Ges. Wiss. Göttingen, 26, 98-100 (1918).

16) Manabe, S., & Fujioka, R.: Thermal molecular motion from 150 to 350 K for regenerated cellulose solids. Polymer Journal, 28, 860-866 (1996).

17) Nielsen, L. E.: Mechanical properties of polymers and composites (Volume 1). New York: Marcel Dekker, Inc., Chapter 4, Section II, 147 (1974).

18) Ferry, J. D.: Viscoelastic properties of polymers. New York: John Wiley & Sons, Chapter 2, Section A9, 47 (1980).

19) Fox, T. G.: Influence of diluent and copolymer composition on the glass transition temperature of a polymer system. Bull. Am. Phys. Soc., 1, 123 (1956).

20) Stuart, A., McCallum, M. M., Fan, D., LeCaptain, D. J., Lee, C. Y., & Mohanty, D. K.: Poly (vinyl chloride) plasticized with succinate esters: synthesis and characterization. Polym. Bull., 65, 589-598 (2010).

21) Szczesniak, L., Rachocki, A., & Tritt-Goc, J.: Glass transition temperature and thermal decomposition of cellulose powder. Cellulose, 15, 445-451 (2008).

22) Zhou, S., Tashiro, K., Hongo, T., Shirataki, H., Yamane, C., & Ii, T.: Influence of water on structure and mechanical properties of regenerated cellulose studied by an organized combination of infrared spectra, X-ray diffraction, and dynamic viscoelastic data measured as functions of temperature and humidity. Macromolecules, 34, 1274–1280 (2001).

23) Yachi, T., Hayashi, J., Takai, M., & Shimizu, U.: Supermolecular structure of cellulose: stepwise decrease in LODP and particle size of cellulose hydrolyzed after chemical treatment. Journal of Applied Polymer Science: Applied Polymer Symposium, 37, 325-343 (1983).

24) Saito, T., Nishiyama, Y., Putaux, J. L., Vignon, M., & Isogai, A.: Homogeneous suspensions of individualized microfibrils from TEMPO-catalyzed oxidation of native cellulose. Biomacromolecules, 7, 1687-1691 (2006).

25) Miyamoto, H., Yamane, C., Mori, M., Okajima, K., & Sugiyama, J.: Cross-sectional distribution of crystalline and fibril orientations of typical regenerated cellulose fibers in reaction to their fibrillation resistance. Textile Research Journal, 79, 694-701 (2009).

26) Langan, P., Nishiyama, Y., & Chanzy, H.: A revised structure and hydrogen bonding system in cellulose II from a neutron fiber diffraction analysis. Journal of American Chemical Society, 121, 9940-9946 (1999).

27) Penttilä, P. A., Altgen, M., Carl, N., Linden, P., Morfin, I., Österberg, M., Schweins, R., & Rautkari, L.: Moisture-related changes in the nanostructure of woods studied with X-ray and neutron scattering. Cellulose, https://doi.org/10.1007/s10570-019-02781-7 (2019).

28) Hermans, P. H., Hermans, J. J., & Vermaas, D.: Density of cellulose fibers. III. density and refractivity of natural fibers and rayon. Journal of Polymer Science, 1(3), 162-171 (1946).

29) Hermans, P. H.: The density and refractivity of cellulose fibers in relation to their structure. J. Text. Inst., 38(2), 63-74 (1947).

Chapter 3. Relaxation phenomenon and swelling behavior of regenerated cellulose fibers affected by organic solvents

3.1. Introduction

Regenerated cellulose fibers are extremely sensitive to water, with home-washing resulting in shrinkage, deep wrinkles and fibrillation, which prevents them from being used for various purposes. The hydrophilicity of cellulose is due to three hydroxyls per glucose unit; however, this alone cannot reasonably explain why its wettability is so high. In order to solve this problem, it is necessary to clarify the influence of water on regenerated cellulose. In Chapter 2, the viscoelastic behavior and small angle X-ray scattering of regenerated cellulose fibers with water regain ranging from 0 to 100% were investigated. It was found that the glass-transition temperature (*T*g) decreased to room temperature at water regains of 78% (rayon), 63% (cupra) and 56% (lyocell), and the small angle two-dimensional scattering intensity of regenerated cellulose fibers with various water regains peaked on the equator line in the wet state and remarkably changed at a water regain of 30%, which suggests that the molecular motion of the main chain of cellulose caused the maximum of equatorial intensity with increasing water regain. These results suggested that water penetrates into amorphous regions between microfibrils and widens the space between them, leading to the micro-Brownian movement of cellulose main chains at the specific water regain. However, cellulose is an intrinsically amphiphilic polymer[1-4]. Why can dry cleaning generally applied to fabrics made of regenerated cellulose fibers avoiding significant wrinkling? It is possible that the regenerated cellulose fibers are affected by organic solvents. In this chapter, to understand these issues, the dynamic viscoelastic behavior caused by organic solvents and the relating swelling phenomenon should be clarified for the regenerated cellulose lyocell. This NMMO-based lyocell process is a closed system that can recover solvent almost quantitatively and has very little pulp loss due to little degradation, which is useful for cost reduction and environmental conservation[5-7]. Thereby, the lyocell process will gradually become a major production system for regenerated cellulose fiber, instead of the rayon process.

3.2. Materials and Methods

3.2.1. Materials

The regenerated cellulose fibers, lyocell (1.7 dtex, Lenzing AG), were used. The next organic solvents as immersion liquid were used: acetone, methanol, ethanol, propanol and butanol as polar solvents, and hexane, heptane, octane, nonane, decane, cyclohexane and petroleum-based dry cleaning solvents (JXTG Nippon Oil & Energy Corporation) as non-polar solvents.

3.2.2. Dynamic Viscoelasticity

The effect of organic solvents on the mechanical loss tangent δ (the ratio of *Er* to loss modulus of the fibers, tan δ) were evaluated using a viscoelastic spectrometer (DVA-200, IT Keisoku Seigyo Co., Ltd., Japan) under the following conditions: frequency, 10 Hz; temperature, 298 K; and sample length, 20 mm. The sample was immersed in solvents for 10 min and extra solvents was removed, then a bundle of the fiber impregnated with a solution was cut into two halves of the same weight. One half was used for viscoelastic measurement. The apparatus was placed in a conditioned room (298 K and 65% RH) and the measuring samples were not sealed to contact with atmospheric air. The other half was simultaneously placed close to the measuring spot and the weight was measured every 15 seconds to determine the time-dependence of solvent regain, and then the time–tan δ curve was changed to a solvent regain–tan δ curve.

3.2.3. Small angle X-ray scattering (SAXS)

In order to investigate the periodicity of the intervals of microfibrils accompanying swelling of regenerated cellulose fibers, small angle two-dimensional scattering images were obtained by high intensity X-ray synchrotron radiation. The bottom of a glass capillary purchased from WSJ-Glas, Müller GmbH, Germany, was broken to make a glass tube. A bundle of fibers was slipped into the glass tube (diameter 3.0 mm, length 80 mm, thickness 0.01 mm), 100 wt% of solvents was added into the glass tube using a micro-

syringe to adjust the solvent regains to the respective values, and the upper and lower ends of the tube were sealed with glue to prevent water evaporation. After the solvent was uniformly dispersed in the fiber bundle, SAXS measurements were conducted at the experimental station of BL-40B in the synchrotron radiation facility, SPring-8, located in Hyogo prefecture, Japan. The wavelength of the incident X-ray was adjusted to 0.1 nm; camera length was 1206.4 mm; irradiation time was 1.0 sec; and the X-ray beam was focused to a point. The intensity of SAXS was detected by imaging plate. The resulting two-dimensional scattering images were scanned on the equator line, and the long periods were estimated from the positions (q: the scattering vector) of the peaks and shoulders observed.

3.3. Results and Discussion

3.3.1. Relaxation phenomenon of regenerated cellulose fibers by organic solvents

The effect of solvent on tan δ was examined at room temperature (298K) by changing the solvent regain of regenerated cellulose fiber (lyocell) during the measurements. Here, the solvent regain is expressed as the weight/weight percentage (w/w %) of solvents in a fiber versus the fiber's dry weight. The peaks of tan δ were observed at room temperature, when the solvent regains of the regenerated cellulose fiber were changed (Figure 3-1, 3-2), similar to their appearance by water described in Chapter 2. The solvent regains of the peaks (SR_{max}) were 25% for methanol, 36% for ethanol, 65% for propanol and 63% for ethanol as polar solvents, and 35% for hexane, 54% for heptane and 54% for octane as non-polar solvents. In addition, peaks were also observed for acetone and cyclohexane, but SR_{max} could not be measured because these solvents were extremely volatile (Table 3-1).

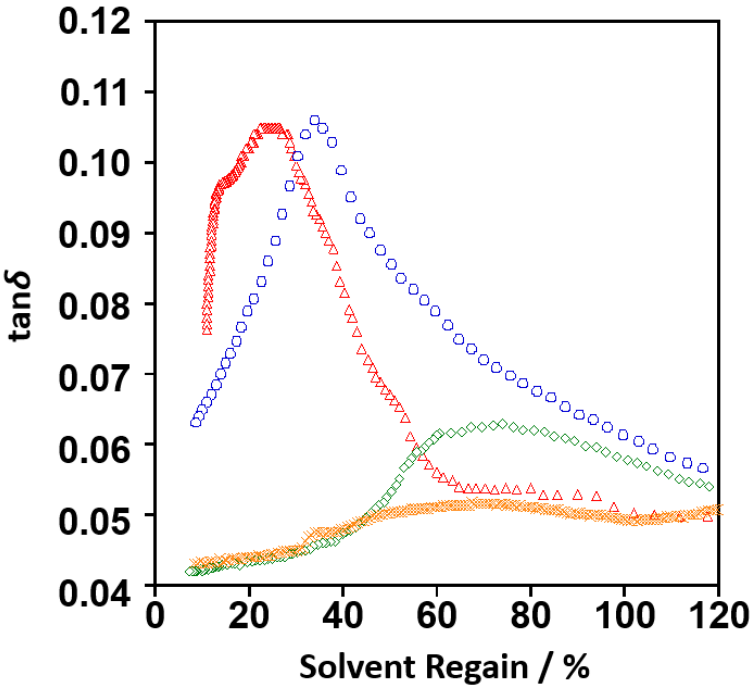

Figure 3-1. Relationship between solvent regain of drying process by regenerated cellulose fiber containing polar solvent and tan δ at 298 K: △, methanol; ○, ethanol; ◇, propanol; ×, butanol.

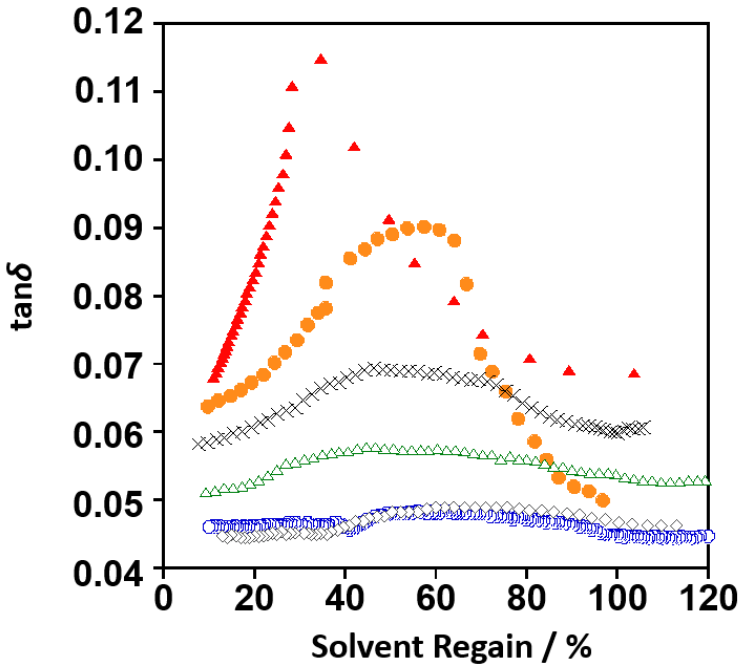

Figure 3-2. Relationship between solvent regain of drying process by regenerated cellulose fiber containing nonpolar solvent and tan δ at 298 K: ▲, hexane; ●, heptane; ×, octane; △, nonane; ○, decane; ◇, dry cleaning solvent.

It was reported that the peaks of the low- and high-temperature regions were assigned to the local segmental motion of cellulose molecules and the micro-Brownian motion of cellulose main chains in amorphous regions[8, 9]. In relation to this high-temperature transition, according to the measurement based on the water regain dependency in Chapter 2, the peaks and shoulder of tan δ are observed when a certain water regain is exceeded (78% rayon, 63% cupra, 56% lyocell) at room temperature, 298K, and it was confirmed that *Tg* was decreased to room temperature. Consequently, it was clarified that when the solvent regain reached to SR_{max}, even with organic solvents, the transition occurred similar to the water regain dependency, and the glass transition temperature of lyocell near 513K in the absolutely dry state was decreased to room temperature by the organic solvent. Based on these results, it was reconfirmed that cellulose is an amphiphilic polymer having hydrophilicity and hydrophobicity.

The SR_{max} at which the glass transition occurs increased as the molecular weight of the solvent increased. The peak heights (tan δ_{max}) at SR_{max} decreased in the order of 0.11 for methanol and ethanol, 0.06 for propanol and 0.05 for butanol as polar solvents, and 0.12 for hexane, 0.09 for heptane and 0.07 for octane as non-polar solvents. In these results, the value of tan δ decreases with increasing molecular weight, suggesting that the size of the moving unit becomes smaller, and the effect on molecular motion is reduced. The values of tan δ_{max} caused by water were in the order of 0.22 for rayon, 0.14 for cupra and 0.11 for lyocell, indicating that the effects of organic solvents were almost the same or lower, and the motion region affected by organic solvents is relatively smaller than that by water.

Table. 3-1 Dynamic absorption and swelling of regenerated cellulose fiber (lyocell) by organic solvents.

Transition	SR_{max}/%	Tan δ_{max}	Swelling ratio/%	Long period/nm
Water	56	0.11	122	6.3
Acetone	-*2	0.08	70	4.2
Methanol	25	0.11	67	5.0
Ethanol	36	0.11	63	4.2
Propanol	65	0.06	79	-*4
Butanol	69	0.05	75	-*4
Cyclohexane	-*2	0.08	50	3.9
Hexane	35	0.12	59	3.7
Heptane	54	0.09	48	-*4
Octane	54	0.07	43	-*4
Nonane	-*3	-*3	43	-*4
Decane	-*3	-*3	37	-*4
Dry cleaning solvent※1	-*3	-*3	-*3	-*4

*1 Petroleum-based solvent mainly composed of nonane and decane. *2 SR_{max} could not be estimated because these solvents were extremely volatile. *3 For alkanes with a molecular weight larger than nonane, almost no tan δ peak or shoulder was observed. *4 Long period could not be estimated because SAXS was not measured for these solvents.

However, in the case of nonane, decane and petroleum-based dry cleaning solvents having large molecular weight (mainly composed of alkanes larger than nonane), almost no tan δ peak or shoulder was observed. This shows that the glass transition of lyocell does not occur in alkane solvents with molecular weight larger than nonane, and does not change from glassy state to so-called rubbery state. When the molecular weight is too large, the solvent may not be able to enter the amorphous region between the microfibrils of regenerated cellulose (lyocell). The same phenomenon was also observed in other regenerated cellulose fibers (cupra and rayon), and no peak or shoulder was observed for alkanes of decane or higher. Thus, in the case of cupra and rayon, it was shown that an alkane solvents larger than nonane does not induce a rubbery state.

As described above, the regenerated cellulose fiber became rubbery state with organic solvents having a low molecular weight, similar to the effects of water. When cellulose is violently rubbed or crumpled and receives intense external force in this state followed by drying into the glassy state, and regenerated cellulose fiber could become wrinkled. However, in the case of alkanes having a molecular weight larger than that of nonane or decane, the regenerated cellulose fiber does not become rubbery and is less likely to wrinkle. Indeed, alkanes with a molecular weight larger than nonane have been empirically specified in petroleum-based dry cleaning solvents, and petroleum-based dry cleaning is basically applied to commercially available regenerated cellulose (rayon, cupra, lyocell). In this study, it was scientifically clarified that these organic solvents were used as dry cleaning solvents, and the reasons why regenerated cellulose fibers cannot be washed with water.

3.3.2. Swelling behavior of regenerated cellulose fibers by organic solvents

Small-angle X-ray scattering images of regenerated cellulose fibers (lyocell) with organic solvents are shown in Figure 3-3. Here, the bundles of fibers were placed vertically. The equatorial intensity of lyocell in hexane appeared to decrease monotonically toward the wide-angle side. The overall intensity increased in the order of cyclohexane, ethanol and acetone, and there seemed to be a maximum for methanol. This intensity became more pronounced in the polar solvent than in the non-polar solvent.

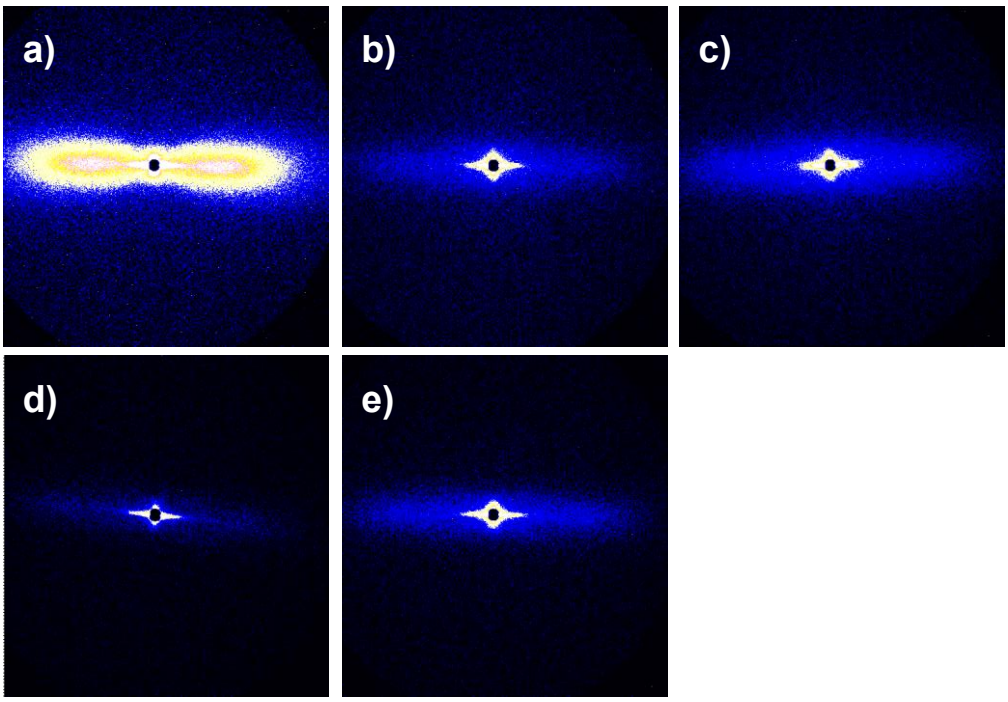

Figure 3-3. Small angle scattering images of regenerated cellulose fiber (lyocell) with various organic solvents: a), methanol; b), ethanol; c), acetone; d), hexane; e), cyclohexane.

Indeed, when the intensity was scanned along the equatorial line, scattering peaks and shoulders were observed (Figure 3-4). These peaks and shoulders became more pronounced for polar solvents and shifted to the low angle side than non-polar solvents. The long periods estimated from the scattering vector q of these peaks and shoulders (Table 3-1), which were 5.0 nm for methanol, 4.2 nm for acetone, 4.2 nm for ethanol, 3.9 nm for cyclohexane and 3.7 nm for hexane. In Chapter 2, the long period of lyocell was

3.4 nm at 0% water regain, and the apparent crystal sizes, which were estimated by Scheller's equation[10], of (110), (020) and ($1\bar{1}0$) were 3.67, 3.52 and 3.64 nm for lyocell, respectively. The microfibrils of regenerated cellulose fibers have been defined by Yachi, Hayashi, Takai, & Shimizu[11] as trains of microcrystals with a width of 3.5 nm and length of 20 nm, connected with each other along the *c* axis direction. In the case of natural cellulose, microfibrils with a width of about 4 nm and also appearing as trains of microcrystals are observed by transmission electron microscopy[12]. The expansion of the long period that represented the existence of microfibrils (microcrystals) was also observed like that in the water regain dependency of the regenerated cellulose fiber in Chapter 2, and it was suggested that the interval of microfibrils expands by wetting. Therefore, the appearance of these scattering peaks or shoulders could be caused by differences in electron density between crystals (density of cellulose II, 1.60 g/cm^3: Langan, Nishiyama, & Chanzy[13]) and inter-crystalline regions where organic solvents

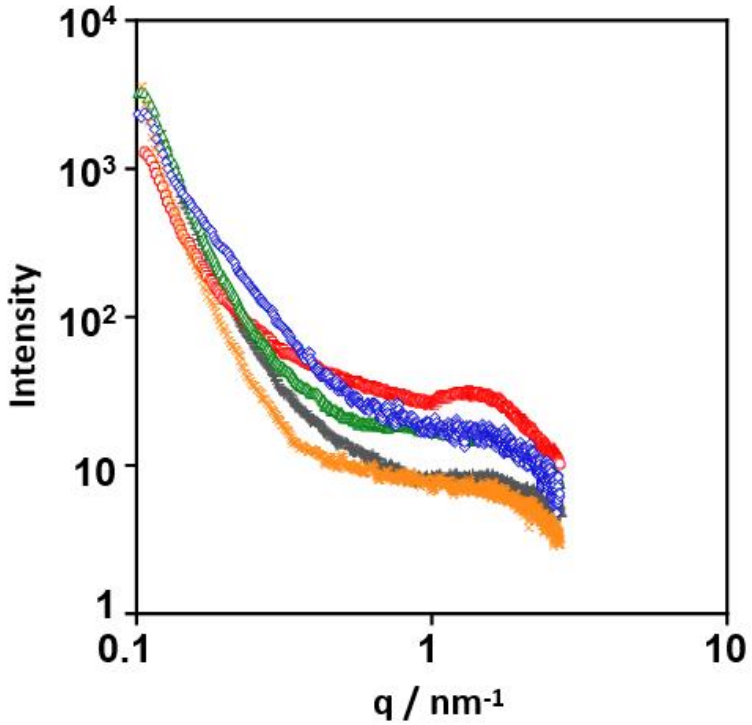

Figure 3-4. Small angle scattering profiles on the equator line of regenerated cellulose fiber (lyocell) with various water regains: ○, methanol; ◇, ethanol; △, acetone; ×, hexane; +, cyclohexane.

with low molecular weight easily penetrate and reduce the density, and the long period could be the distance between microfibrils, which is schematically depicted in Figure 2-8. For this reason, it is presumed that, as the solvent regain of the organic solvent increases, the scattering peak or shoulder becomes conspicuous and the long period representing the microfibrils interval widens. The impregnation of the organic solvent also showed similar behavior to the wetting with water, indicating that the organic solvent could widen the presence period of microfibrils.

The swelling ratio of lyocell by measurement was 122% for water, which is remarkably high, 70% for acetone, 67% for methanol, 63% for ethanol, 79% for propanol and 75% for butanol as polar solvents, and 59% for hexane, 48% for heptane, 43% for nonane and 37% for decane as non-polar solvents. The swelling ratio is defined as the ratio of the weight/weight percentage (w/w%) of solvents that remains in fibers after centrifugation at 1,000 × g, to dry weight. This value was lower in non-polar solvents than in polar solvents, and decreased with increasing molecular weight in non-polar solvents. This corresponded to the long period of lyocell, and is larger for polar solvents than for non-polar solvents. It could be related to the relaxation phenomenon described above; as the molecular weight increased, the SR_{max} increased and the tan δ_{max} indicating the size of the molecular motion region decreased. These changes in long period and swelling degree were also observed in other regenerated cellulose fibers (cupra).

The changes in viscoelastic behavior and structures caused by organic solvents can be summarized as follows. Initially, small amount of organic solvents penetrates into the dry space among microfibrils. However, overall molecular movement of the cellulose backbone has not yet occurred at this stage. When organic solvents further infiltrate into the regions, the solvent regain reaches SR_{max} (25% for methanol, 36% for ethanol, 65% for propanol and 69% for butanol as polar solvents, and 35% for hexane, 54% for heptane and 54% for octane as non-polar solvents) where the peaks of tan δ appear. In this state, the main chain of the cellulose molecule starts to move and the regenerated cellulose fibers change to a so-called rubbery state. Meanwhile, no peak showing glass transition appears

in nonane, decane or dry cleaning solvents with high molecular weight alkanes, suggesting that non-polar solvents with high molecular weight cannot penetrate gaps of microfibrils and molecular motion does not occur, meaning that the regenerated cellulose could not become rubbery. Accordingly, regenerated cellulose fiber can be treated with petroleum-based dry cleaning, while washing with water causes significant wrinkles.

3.4. Conclusions

Tan δ peaks were observed in tan δ-solvent regain curves at SR_{max}; 25% for methanol, 36% for ethanol, 65% for propanol and 69% for butanol as polar solvents, and 35% for hexane, 54% for heptane and 54% for octane as non-polar solvents at room temperature. As a result, it was clarified that the regenerated cellulose fiber showed the same phenomenon as glass transition by water (78% rayon, 63% cupra, 56% lyocell), for both non-polar and polar solvents. The tan δ_{max} decreased with increasing molecular weight; 0.11 for methanol and ethanol, 0.06 for propanol and 0.05 for butanol as polar solvents, and 0.12 for hexane, 0.09 for heptane and 0.07 for octane as non-polar solvents. This suggests that molecular motion is suppressed by high molecular weight solvents. The peak of tan δ was lower than the effect of water, and this indicates that the size of motion region for the organic solvent is smaller. Nevertheless, this also shows that organic solvents increased the volume of moving units as compared to the dry state by loosening intermolecular forces and widening the space between cellulose molecules. SAXS showed the maxima and shoulders on the equator line, suggesting that organic solvents decreased the density of the amorphous region, i.e., widened the space between cellulose molecules, creating sufficient space for the micro-Brownian motion of cellulose main chains. However, alkanes having a molecular weight larger than nonane did not show tan δ peaks, which suggests that the cellulose will not become rubbery as the solvent cannot enter between microfibrils. These results revealed the reason that the regenerated cellulose fibers can be washed by petroleum-based dry cleaning solvent, while washing with water causes significant wrinkles. Why can natural fibers, which are composed of the same cellulose fibers, such as cotton and linen, be washed with water? In Chapter 4, the dynamic viscoelastic behavior caused by water and the relating swelling phenomenon of natural cellulose will be clarified.

References

1) Lindman, B., Karlström, G., & Stigsson, L.: On the mechanism of dissolution of cellulose, J. Mol. Liq., 156, 76-81 (2010).

2) Medronho, B., Romano, A., Miguel, M.G., Stigsson, L., & Lindman B.: Rationalizing cellulose (in) solubility: reviewing basic physicochemical aspects and role of hydrophobic interactions, Cellulose, 19, 581-587 (2012).

3) Medronho, B., & Lindman, B.: Brief overview on cellulose dissolution/ regeneration interactions and mechanisms, Adv. colloid and interf. sci., DOI: 10.1016/j.cis.2014.05.004 (2014).

4) Medronho, B., & Lindman, B.: Competing forces during cellulose dissolution: From solvents to mechanisms, Curr. Opin. Colloid Interface Sci, 19, 32-40 (2014).

5) Firgo, H., Eibl, M., Kalt, W., & Meister, G.: Critical questions related to the future of the NMMO technology, Lenz. Ber. 74, 81-89 (1994).

6) Firgo, H., Eibl, M., & Eichinger, D.: Lyocell - an ecological alternative, Lenz. Ber. 75, 47-50 (1995).

7) Marini, I., Firgo, H., & Eibl, M.: Lenzing Lyocell, Lenz. Ber. 74, 53-56 (1994).

8) Manabe, S., & Fujioka, R.: Thermal molecular motion from 150 to 350 K for regenerated cellulose solids. Polymer Journal, 28, 860-866 (1996).

9) Yamane, C., Mori, M., Saito, M., & Okajima, K.: Structures and mechanical properties of cellulose filament spun from cellulose/aqueous NaOH solution system. Polymer Journal, 28, 1039-1047 (1996).

10) Scherrer, P. (1918). Determination of the size and internal structure of colloidal particles using X-rays. Nachr. Ges. Wiss. Göttingen, 26, 98-100.

11) Yachi, T., Hayashi, J., Takai, M., & Shimizu, U.: Supermolecular structure of cellulose: stepwise decrease in LODP and particle size of cellulose hydrolyzed after chemical treatment. Journal of Applied Polymer Science: Applied Polymer Symposium, 37, 325-343 (1983).

12) Saito, T., Nishiyama, Y., Putaux, J. L., Vignon, M., & Isogai, A.: Homogeneous

suspensions of individualized microfibrils from TEMPO-catalyzed oxidation of native cellulose. Biomacromolecules, 7, 1687-1691 (2006).

13) Langan, P., Nishiyama, Y., & Chanzy, H.: A revised structure and hydrogen bonding system in cellulose II from a neutron fiber diffraction analysis. Journal of American Chemical Society, 121, 9940-9946 (1999).

Chapter 4. Relaxation phenomenon and swelling behavior of natural cellulose fibers affected by water

4.1. Introduction

Cellulose precipitated from cellulose solution by non-solvents is classified as regenerated cellulose and is used in many fields, such as textile fibers, cellophane films, cellulose sponges and meat casings. However, its higher wettability prevents the expansion of its applications. The production ratio of man-made cellulose fibers including acetate fibers to global fiber production was approximately 6% in 2017. Regenerated cellulose fibers are extremely sensitive to water, with home-washing resulting in shrinkage, deep wrinkles and fibrillation, which usually requires them to be dry-cleaned, and prevents them from being used for various purposes. The hydrophilicity of cellulose is due to three hydroxyls per glucose unit; however, this alone cannot reasonably explain why wettability of regenerated cellulose is so high. To understand these issues, the dynamic viscoelastic behavior caused by water and the relating swelling phenomenon should be clarified. In Chapter 2, we examined the effect of water on regenerated cellulose fibers with respect to the relaxation phenomenon and swelling behavior. The mechanical loss tangent δ (tan δ) peaks and shoulder were observed at room temperature in the wet state. At the same time, the storage modulus markedly decreased around these water regains. This suggests that glass transition temperatures of 513-552 K would be shifted to room temperature by water. Small angle X-ray scattering showed the maxima and shoulders in the wet state, which suggested that water decreased the density of the amorphous region and made space for the movement of polymer segments. These results suggest that water penetrates into amorphous regions between microfibrils and widens the space between them, leading to the micro-Brownian movement of cellulose main chains at the specific water regain. On the other hand, cellulose is an intrinsically amphiphilic polymer[1-4]. In Chapter 3, the dynamic viscoelastic behavior caused by organic solvents and the relating swelling phenomenon were clarified. The glass transition by organic solvents such as hexane,

heptane, octane, ethanol and acetone, was observed, although the peaks of tan δ were low, which suggested the regions affected by the organic solvents are small. In contrast, the tan δ profiles were flat in alkanes with larger molecular weight than nonane and in dry cleaning solvent (mainly composed of alkanes larger than nonane), which suggests that as molecular weight increases, the effect of the solvents on molecular motion decreases. Even for natural cellulose, however, wrinkles and swelling shrinkage due to washing with water are known to occur. It is possible that natural cellulose also has some transitions caused by water, similar to regenerated cellulose. To understand these issues, the dynamic viscoelastic behavior of natural cellulose caused by water and the related swelling phenomenon will be clarified in this chapter.

4.2. Materials and Methods

4.2.1. Materials

Two kinds of natural cellulose fibers were used: cotton (PIMA, 4.8 dtex, Omikenshi Co., Ltd.); ramie (6.5 dtex, Tanakanao Senryoten Co., Ltd.).

4.2.2. Dynamic Viscoelasticity

The effect of water regains on the storage modulus (*Er*) and tan δ were evaluated using a viscoelastic spectrometer (DVA-200, IT Keisoku Seigyo Co., Ltd., Japan) under the following conditions: frequency, 10 Hz; temperature, 298 K; and sample length, 20 mm. The sample was immersed in water for 10 min and extra water was removed, then the wet fiber bundle was cut into two halves of the same weight. One half was used for viscoelastic measurement. The apparatus was placed in a conditioned room (298 K and 65% RH) and the measuring samples were not sealed to contact with atmospheric air. The other half was simultaneously placed close to the measuring spot and the weight was measured every 30 seconds to determine the time-dependence of water regain, and then the time–tan δ curve was changed to a water regain–tan δ curve.

4.2.3. Small angle X-ray scattering (SAXS)

In order to investigate the periodicity of the intervals of microfibrils accompanying swelling of natural cellulose fibers, small angle two-dimensional scattering images were obtained by high intensity X-ray synchrotron radiation. The bottom of a glass capillary purchased from WSJ-Glas, Müller GmbH, Germany, was broken to make a glass tube. A bundle of fibers was slipped into the glass tube (diameter 3.0 mm, length 80 mm, thickness 0.01 mm), a specific amount of water was added into the glass tube using a micro-syringe to adjust the water regains to the respective values, and the upper and lower ends of the tube were sealed with glue to prevent water evaporation. After the water was uniformly dispersed in the fiber bundle, SAXS measurements were conducted at the experimental station of BL-40B in the synchrotron radiation facility, SPring-8, located in Hyogo

prefecture, Japan. The wavelength of the incident X-ray was adjusted to 0.1 nm; camera length was 1206.4 mm; irradiation time was 1.0 sec; and the X-ray beam was focused to a point. The intensity of SAXS was detected by imaging plate. The resulting two-dimensional scattering images were scanned on the equator line, and the long periods were estimated from the positions (q: the scattering vector) of the peaks and shoulders observed.

4.3. Results and Discussion

4.3.1. Relaxation phenomenon of natural cellulose fibers

The water dependency of tan δ was examined at room temperature (298K) by changing the water regain of natural cellulose fibers (cotton and ramie) during the measurements. Here, the water regain is expressed as the weight/weight percentage (w/w %) of water in a fiber versus the fiber's dry weight. The peaks of tan δ were observed at room temperature, when the water regains of the natural cellulose fiber were changed (Figure 4-1), similar to their appearance for regenerated cellulose fibers in the measurements of water and organic solvent regain dependency in Chapters 2 and 3.

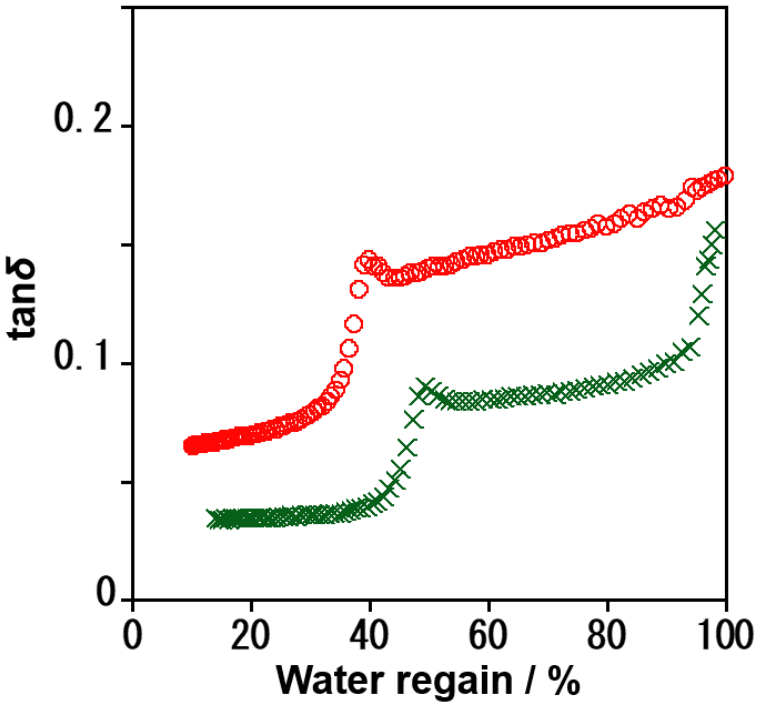

Figure 4-1. Relationship between water regain of natural cellulose fibers and viscoelastic parameter tan δ at 298 K: ○, cotton; ×, ramie.

The water regains of the peaks (WR_{max}) were 39% for cotton and 49% for ramie. It was reported that the peaks of the low- and high-temperature regions were assigned to the local segmental motion of cellulose molecules and the micro-Brownian motion of cellulose main chains in amorphous regions[5, 6]. In relation to this high-temperature

transition, according to the measurement based on the water regain dependency in Chapter 2, the peaks and shoulder of tan δ are observed when a certain water regain is exceeded (78% rayon, 63% cupra, 56% lyocell) at room temperature, 298K, and it is suggested that *T*g was decreased to room temperature. Consequently, it was suggested that when water regain reaches WR_{max}, the transition of natural cellulose occurs similar to the regenerated cellulose. The natural cellulose fibers could also enter a so-called rubbery state in the wet state. The peak heights (tan δ_{max}) at WR_{max} were 0.14 for cotton and 0.09 for ramie. The values of tan δ_{max} for regenerated cellulose fibers were in the order of 0.22 for rayon, 0.14 for cupra and 0.11 for lyocell, indicating that the effect of water on natural cellulose fibers was similar to or lower than that on regenerated cellulose fibers, and the size of motion region affected by water is similar to or lower than that of regenerated cellulose. The storage modulus *Er* decreased sharply with increasing water regain until the regain reached WR_{max}, and then levelled off; the values for cotton and ramie were 1/2 and 7/10, respectively, as compared to their starting values (Figure 4-2).

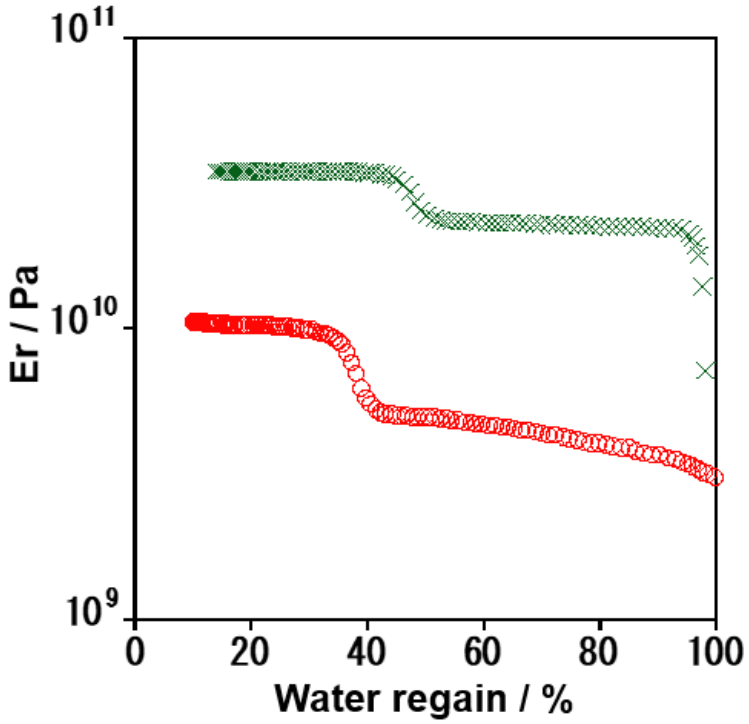

Figure 4-2. Relationship between water regain of natural cellulose fibers and *Er* (Pa) at 298K: ○, cotton; ×, ramie.

The degree of reduction (1/2, 7/10) for natural cellulose was less than that for regenerated cellulose fibers (1/10 for rayon, 1/10 for cupra, 3/10 for lyocell) in Chapter 2. Although the natural cellulose fiber essentially changed to a rubbery state, the effect of water was small, as judged by slight change in *Er* by wetting. In addition, the water regains at a room temperature of 298 K and relative humidity of 100% (hereinafter referred to as saturated water regain) were 26% for cotton and 20% for ramie. This indicates that the water regain of natural cellulose cannot reach WR_{max} under high humidity conditions in daily life. This suggests that adding a small amount of water puts natural cellulose into the rubbery state. The natural cellulose fibers are wrinkled by home-washing, as we experience in daily life. However, it is possible that natural cellulose fiber is less likely to wrinkle because the decrease in elastic modulus is less then regenerated cellulose fibers.

4.3.2. Swelling behavior of natural cellulose fibers

Small-angle X-ray scattering images of natural cellulose fibers with water are shown in Figures 4-3 for cotton and 4-4 for ramie. Here, the bundles of fibers were placed vertically. The equatorial intensity at water regains of 0% and 8% for cotton and 0% and 12% for ramie appeared to decrease monotonically toward the wide-angle side. As the water regains increased, the overall intensity increased, and there seemed to be a maximum or shoulders at over 30% water regains. Indeed, when the intensity was scanned along the equatorial line, scattering shoulders were observed (Figure 4-5 for cotton, 4-6 for ramie).

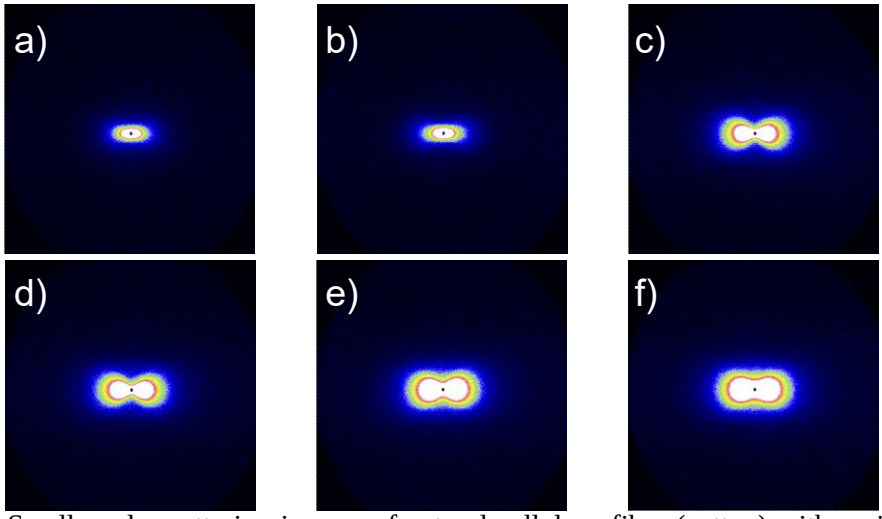

Figure 4-3. Small angle scattering images of natural cellulose fiber (cotton) with various water regains: a), 0%; b), 8%; c), 30%; d), 50%; e), 75%; f), 100%.

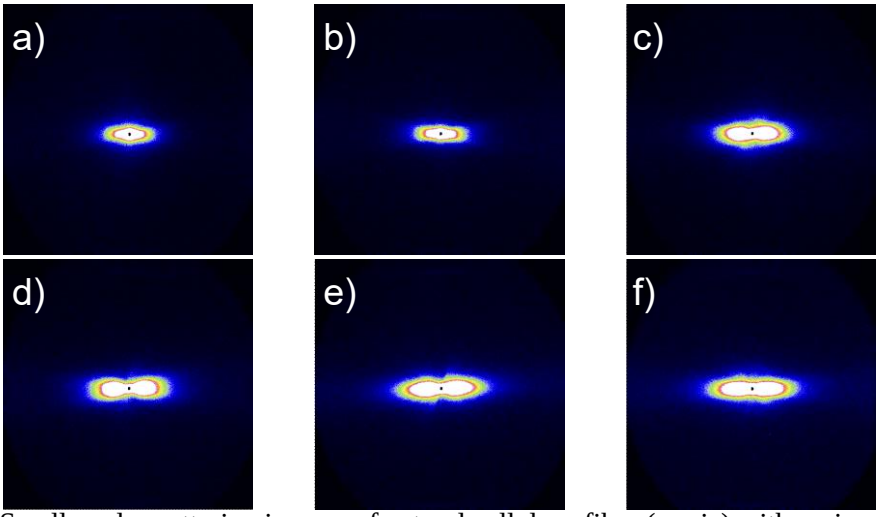

Figure 4-4. Small angle scattering images of natural cellulose fiber (ramie) with various water regains: a), 0%; b), 12%; c), 30%; d), 50%; e), 75, f), 100%.

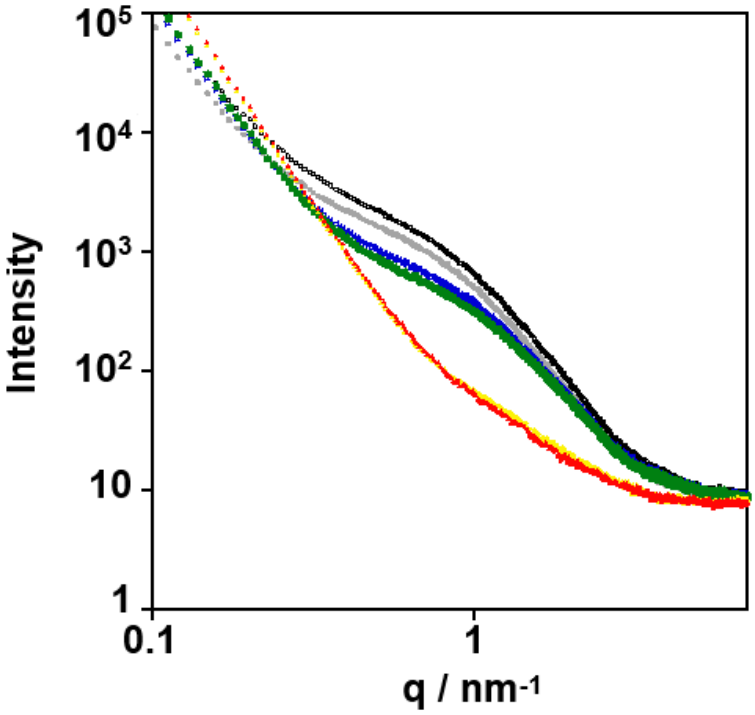

Figure 4-5. Small angle scattering profiles on the equator line of cotton with various water regains: ○, 100%; ●, 75%; □, 50%; ■, 30%; △, 8%; ▲, 0%.

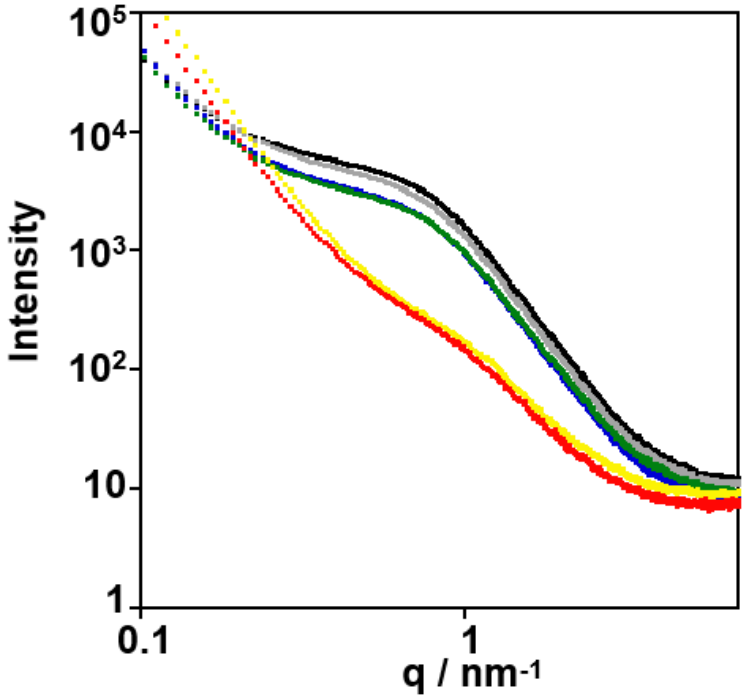

Figure 4-6. Small angle scattering profiles on the equator line of ramie with various water regains: ○, 100%; ●, 75%; □, 50%; ■, 30%; △, 12%; ▲, 0%.

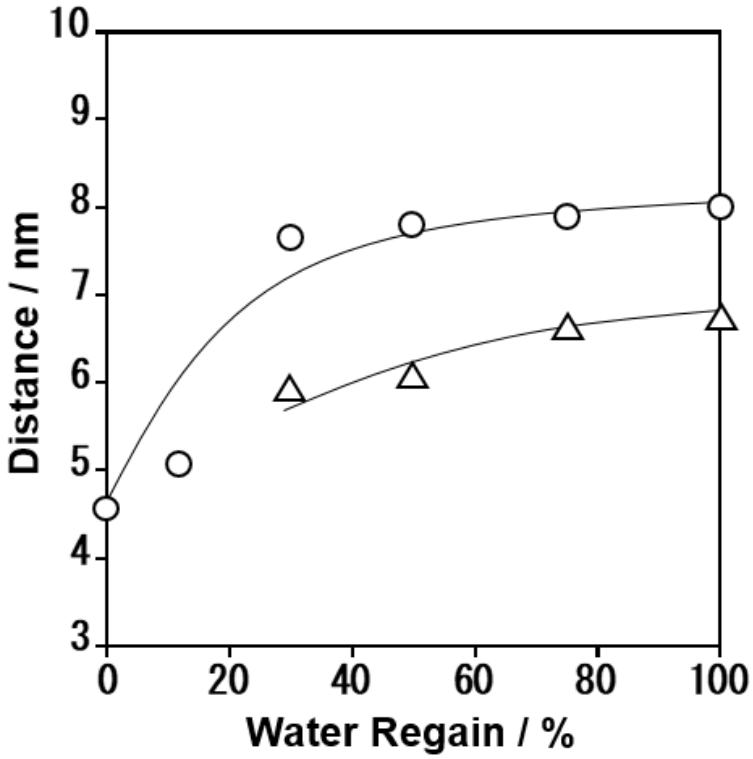

Figure 4-7. Long periods of regenerated cellulose fibers with various water regains: △, cotton; ○, ramie.

These shoulders became more pronounced with increasing water regains, and shifted to the low angle side. The long periods estimated from the scattering vector *q* of these shoulders, which were water regains of 30% for 5.9 nm, 50% for 6.0 nm, 75% for 6.6 nm, 100% for 6.7 nm for 100% for cotton, and 0% for 4.6 nm, 12% for 5.1 nm, 30% for 7.6 nm, 50% for 7.8 nm, 75% for 7.9 nm, 100% for 8.0 nm for ramie. There were no data plots at 0% and 8% for cotton due to the absence of scattering peaks or shoulders; however, when the line was extrapolated to 0%, the long period of 0% appeared to be about 4.5 nm. The long periods extended with increasing water regain in both natural cellulose fibers. The long periods of cotton and ramie seemed to level off for water regains higher than WR_{max}. This corresponded to the changes in *Er*, which also leveled-off in the same region of water regain. These results suggested that the changes in long periods caused by water could be related to the relaxation phenomenon. In the study on water

regain dependency of regenerated cellulose fiber in Chapter 2, the long period that reveals the existence period of microfibrils was 3.4 nm in the dry state, and it was reported that the interval of microfibrils increases with wetting. It was suggested that the same behavior was observed in natural cellulose fibers. Indeed, in the case of natural cellulose, microfibrils with a width of about 4 nm and also appearing as trains of microcrystals are observed by transmission electron microscopy[7]. The long period of dry cotton and ramie were about 4.5 nm estimated by *q* of the shoulders. Therefore, the appearance of these scattering shoulders could be caused by differences in electron density between crystals (density of cellulose II, 1.60 g/cm^3: Langan, Nishiyama, & Chanzy[8]) and inter-crystalline regions where water easily penetrates and reduces the density, and the long period could be the distance between microfibrils, which is schematically depicted in Figure 2-8. The shoulders of ramie with 0% and 12% water regains were extremely small (Figure 4-6) and there were no shoulders for cotton with 0% and 8% water regains (Figure 4-5). This suggests that there is almost no difference between the density of microfibrils and that of inter-microfibrils in the dry state. Indeed, Hermans et al.[9, 10] reported that the density of amorphous regions of regenerated cellulose was slightly lower, by only 6%, when compared with crystals.

The changes in physical properties and structures caused by water can be summarized as follows. Initially, water penetrates into the dry space among microfibrils to lower the *Er* and widen that region. Subsequently, the water regain reaches saturated water regain (cotton, 26%; ramie, 20%). However, overall molecular movement of the cellulose backbone has not yet occurred. When water further infiltrates into the regions; changes in *Er* and the distance between microfibrils are leveled off; and the water regain reaches WR_{max} (cotton, 39%; ramie, 49%) where the peaks of tan δ appear. In this state, the main chain of the cellulose molecule starts to move and natural cellulose fibers also change to a so-called rubbery state. In this state, crumpling and rubbing by a washing machine in water, where natural cellulose becomes rubbery, followed by drying into the glassy state, could be the main reason for wrinkles during home washing. However, in the

case of natural cellulose, these wrinkles were lather weak comparing to those of regenerated fibers and can be eliminated to some extent by rewetting and ironing after drying. Therefore, natural cellulose fibers are less affected by water and are able to withstand washing with water.

4.4. Conclusions

Tan δ peaks were observed in tan δ-water regain curves at WR_{max}; 39% for cotton and 49% for ramie at room temperature. *Er* markedly decreased around these water regains. It is possible that the mechanical absorption is due to micro-Brownian movement of the cellulose main chains. Even in the amorphous region, a portion of cellulose chains builds up intra- and intermolecular hydrogen bonds, which may make the occurrence of micro-Brownian motion difficult at low temperatures. Water probably weakens the hydrogen bonds and widens the space of the amorphous region, resulting in a marked decrease in the glass transition temperature. The order of tan δ_{max} among the fibers was not the same as that of WR_{max}; 0.14 for cotton and 0.09 for ramie, indicating that ramie would have the smallest-sized moving unit, followed by cotton and regenerated cellulose, except for lyocell (0.22 for rayon, 0.14 for cupra and 0.11 for lyocell). The decreases in *Er* with natural cellulose (1/2 for cotton, 7/10 for ramie) were smaller than those with regenerated cellulose (1/10 for rayon, 1/10 for cupra, 3/10 for lyocell). SAXS showed shoulders on the equator line in the wet state, suggesting that water decreased the density of the amorphous region, i.e., widened the space between cellulose molecules, creating sufficient space for the micro-Brownian motion of cellulose main chains. Therefore, natural cellulose is wrinkled similar to regenerated cellulose due to washing by water. However, in the case of natural cellulose, these wrinkles can be eliminated to some extent by rewetting and ironing after drying. This suggests that if the molecular movement of regenerated cellulose was reduced to the same level as natural cellulose fiber, the intrinsic problem of regenerated cellulose fiber could be resolved; and then, the post-treatments for natural cellulose fibers to reduce the effects of water could be applied to regenerated cellulose fibers, and regenerated cellulose fibers could be used like cotton.

References

1) Lindman, B., Karlström, G., & Stigsson, L.: On the mechanism of dissolution of cellulose, J. Mol. Liq., 156, 76-81 (2010).

2) Medronho, B., Romano, A., Miguel, M.G., Stigsson, L., & Lindman B.: Rationalizing cellulose (in) solubility: reviewing basic physicochemical aspects and role of hydrophobic interactions, Cellulose, 19, 581-587 (2012).

3) Medronho, B., & Lindman, B.: Brief overview on cellulose dissolution/ regeneration interactions and mechanisms, Adv. colloid and interf. sci., DOI: 10.1016/j.cis.2014.05.004 (2014).

4) Medronho, B., & Lindman, B.: Competing forces during cellulose dissolution: From solvents to mechanisms, Curr. Opin. Colloid Interface Sci, 19, 32-40 (2014).

5) Manabe, S., & Fujioka, R.: Thermal molecular motion from 150 to 350 K for regenerated cellulose solids. Polymer Journal, 28, 860-866 (1996).

6) Yamane, C., Mori, M., Saito, M., & Okajima, K.: Structures and mechanical properties of cellulose filament spun from cellulose/aqueous NaOH solution system. Polymer Journal, 28, 1039-1047 (1996).

7) Saito, T., Nishiyama, Y., Putaux, J. L., Vignon, M., & Isogai, A.: Homogeneous suspensions of individualized microfibrils from TEMPO-catalyzed oxidation of native cellulose. Biomacromolecules, 7, 1687-1691 (2006).

8) Langan, P., Nishiyama, Y., & Chanzy, H.: A revised structure and hydrogen bonding system in cellulose II from a neutron fiber diffraction analysis. Journal of American Chemical Society, 121, 9940-9946 (1999).

9) Hermans, P. H., Hermans, J. J., & Vermaas, D.: Density of cellulose fibers. III. density and refractivity of natural fibers and rayon. Journal of Polymer Science, 1(3), 162-171 (1946).

10) Hermans, P. H.: The density and refractivity of cellulose fibers in relation to their structure. J. Text. Inst., 38(2), 63-74 (1947).

Chapter 5. Conclusion

Regenerated cellulose has been identified as one of the most hydrophilic polymers. The higher wettability prevents the expansion of its applications. The commercially available regenerated cellulose fibers are rayon, cupra and lyocell, and are prepared from cellulose solutions of CS_2/aqueous NaOH, Cu/aqueous NH_3 and *N*-methyl morpholine *N*-oxide (NMMO), respectively. When fabrics made of regenerated cellulose fibers are washed with water, wrinkling, shrinking and fibrillation occur, which usually requires them to be dry-cleaned. In order to solve these problems and develop advantageous points, it is necessary to clarify the influence of water on regenerated cellulose. In this study, the effects of water and organic solvents on relaxation phenomenon and swelling behavior of natural and regenerated cellulose fibers were examined.

In Chapter 2, the dynamic viscoelastic behavior caused by water and the relating swelling phenomenon were clarified. Molecular movements of cellulose main chains caused by water are the essence of the problems. It was clarified that the glass transition temperature (*T*g) of dry regenerated cellulose (rayon 552 K, cupra 523 K, lyocell 513 K) decreases to room temperature by water. The water regains of the tan δ peaks and shoulder (WR_{max}) were 78% for rayon, 63% for cupra, and 56% for lyocell. It is possible that the mechanical absorption is due to micro-Brownian movement of the cellulose main chains. The values of peak heights (tan δ_{max}) caused by water were in the order of 0.22 for rayon, 0.14 for cupra and 0.11 for lyocell, which was the same order as for tan δ_{max} caused by thermal transition; 0.082 for rayon, 0.070 for cupra and 0.056 for lyocell. This indicates that water increased the volume of moving units by weakening intermolecular forces and widening the space between cellulose molecules, also indicating that rayon would have the largest-sized moving unit, followed by cupra and lyocell. Small-angle X-ray scattering (SAXS) showed the maxima and shoulders on the equator line in the wet state, suggesting that water decreased the density of the amorphous region, i.e., widened the space between cellulose molecules, creating sufficient space for the micro-Brownian motion of cellulose

main chains.

In Chapter 3, the dynamic viscoelastic behavior caused by organic solvents and the related swelling phenomenon were clarified. Tan δ peaks were observed with both polar and non-polar solvents in tan δ-solvent regain curves at SR_{max}; 25% for methanol, 36% for ethanol, 65% for propanol and 69% for butanol as polar solvents, and 35% for hexane, 54% for heptane and 54% for octane as non-polar solvents at room temperature. It was clarified that the regenerated cellulose fiber showed the same phenomenon as glass transition by water (78% rayon, 63% cupra, 56% lyocell). The peak of tan δ was lower than with water, and this indicates that the size of motion region of the organic solvent is smaller. This also shows that organic solvents increased the volume of moving units when compared with the dry state by loosening intermolecular forces and widening the space between cellulose molecules. These results reconfirmed that cellulose is an amphiphilic polymer having both hydrophilicity and hydrophobicity. However, an alkane solvent having a molecular weight larger than nonane did not induce these peaks, which suggests that cellulose molecules do not enter a rubbery state, as the solvent cannot enter the space between microfibrils. In addition, the peak heights (tan δ_{max}) at SR_{max} decreased in the order of 0.11 for methanol and ethanol, 0.06 for propanol and 0.05 for butanol as polar solvents, and 0.12 for hexane, 0.09 for heptane, 0.07 for octane as non-polar solvents. In these results, the value of tan δ decreases with increasing molecular weight, suggesting that the size of movement region becomes smaller, and the effect on molecular motion is reduced. The values of tan δ_{max} caused by water were in the order of 0.22 for rayon, 0.14 for cupra and 0.11 for lyocell, indicating that the effect of organic solvents was similar to or lower than that of water; in other words, the motion region affected by organic solvents is smaller than that affected by water. Accordingly, regenerated cellulose fibers can be treated with petroleum-based dry cleaning, while washing with water causes significant wrinkles.

In Chapter 4, the dynamic viscoelastic behavior of natural cellulose caused by water and the related swelling phenomenon were clarified. Tan δ peaks were observed in tan δ-

water regain curves at WR_{max}; 39% for cotton and 49% for ramie at room temperature. *Er* markedly decreased around these water regains. The order of tan δ_{max} for the two fibers was not the same as that of WR_{max}; 0.14 for cotton and 0.09 for ramie, indicating that ramie would have the smallest-sized moving unit, followed by cotton and regenerated cellulose, except lyocell (rayon, 0.22; cupra, 0.14; lyocell, 0.11). The decreasing of *Er* with natural cellulose (cotton, 1/2; ramie, 7/10) was smaller than that of regenerated cellulose (rayon, 1/10; cupra, 1/10; lyocell, 3/10). SAXS showed shoulders on the equator line in the wet state, suggesting that water decreased the density of the amorphous region, i.e., widened the space between cellulose molecules, creating sufficient space for the micro-Brownian motion of cellulose main chains. Therefore, natural cellulose is wrinkled by home-washing, as experienced in daily life. However, in the case of natural cellulose, these wrinkles are weak comparing to those of regenerated fibers and can be eliminated to some extent by rewetting and ironing after drying. This suggests that if the molecular movement of regenerated cellulose was reduced to the same level as in natural cellulose fiber, the inherent problem with regenerated cellulose fibers could be resolved; and then, the post-treatments for natural cellulose fibers to reduce the effects of water could be applied to regenerated cellulose fibers, and regenerated cellulose fibers could be used like cotton.

The changes in physical properties and structures can be summarized as follows. Initially, water and organic solvents except nonane and decane penetrate into the dry space among microfibrils to lower the *Er* and widen that region. Subsequently, in the case of water, the water regains reach the saturated water regain (rayon, 47%; cupra, 37%; lyocell, 31%). At this stage, overall molecular movement of the cellulose backbone has not yet occurred. When water or solvents except nonane and decane further infiltrates into the regions; changes in *Er* and the distance between microfibrils level off; and when the water and solvent regain reaches WR_{max} (rayon, 78%; cupra, 63%; lyocell, 56%) and SR_{max} (methanol, 25%; ethanol, 36%; propanol 65%; butanol 69% as polar solvents: hexane, 35%; heptane, 54%; octane, 54% as non-polar solvents), the peaks or shoulder of tan δ

appear. In this state, the main chain of the cellulose molecule starts to move and the regenerated cellulose fibers change to a so-called rubbery state by water and solvents. However, alkanes with larger molecular weight than nonane cannot penetrate gaps of microfibrils and molecular motion does not occur, as judged by the absence of tan δ_{max} peaks. Accordingly, regenerated cellulose fibers can be treated with petroleum-based dry cleaning, while washing with water causes significant wrinkles. The transition might require sufficient space for movement of cellulose main chains. In the case of natural cellulose, these wrinkles are weak comparing to those of regenerated fibers and can be eliminated to some extent by rewetting and ironing after drying, as the decrease in *Er* by water is low for natural cellulose (cotton, 1/2; ramie, 7/10), when compared to that for regenerated cellulose (rayon, 1/10; cupra, 1/10; lyocell, 3/10). Based on the abovementioned results, it is possible that the glass transition cannot be completely eliminated; however, the post-treatments including resin-process prevent natural cellulose fibers from wrinkle. The dynamic viscoelastic behavior caused by water and the related swelling phenomenon of regenerated cellulose with the post-treatments should be clarified, in addition to other natural fibers such as silk and wool which have not been examined yet by the methods described in this thesis and the expected findings will lead to solve the inherent problems associated with regenerated cellulose fibers.

List of publication

Okugawa, A., Sakaino, M., Yuguchi, Y. and Yamane, C.: Relaxation phenomenon and swelling behavior of regenerated cellulose fibers affected by water, Carbohydrate Polymers, 231, Available online 23 November 2019. DOI: 10.1016/j.carbpol.2019.115663

Reference publication

Okugawa, A., Ishihara, K., Taniguchi, H., Kono, H. and Yamane, C.: In vivo decomposition of ^{13}C labeled regenerated cellulose by the mouse, Cellulose, Available online 2 January 2020. DOI: 10.1007/s10570-020-02968-3

Acknowledgments

I wish to express my gratitude to my supervisor, Prof. Dr. Chihiro Yamane (Graduate School of Home Economics, Kobe Women's University, Hyogo, Japan) for his valuable instructions.

I would like to thank Prof. Dr. Yoshiaki Yuguchi (Osaka Electro Communication University, Osaka, Japan), Prof. Dr. Hiroki Murase (Kyouritsu Women's University, Tokyo, Japan), Manami Sakaino (Graduate School of Home Economics, Kobe Women's University, Hyogo, Japan) for helping with the SAXS measurement and its analysis. The synchrotron radiation experiments were performed at the BL40B2 of SPring-8 with the approval of the Japan Synchrotron Radiation Research Institute.

Special thanks to all members of Kobe Women's University and Cellulose Society of Japan for their support.